DINCEL STRUCTURAL WALLING

USE OF AS3600 – EUROCODE FOR DINCEL WALLS

Analyses and Testing of Dincel Wall System Subjected to Severe Earthquake Loads

By Professor Bijan Samali

Professor of Structural Engineering, School of Civil and Environmental Engineering
Specialist Consultant- accessUTS Pty Ltd

February 2011

Table of Contents

Acknowledgment

The author wishes to acknowledge the valuable assistance of the following people in conducting Finite element analyses, designing test procedures and support systems, fabrication and testing of specimens and reporting.

Dr Shami Nejadi and Mr Vitali Bebekh – for structural analyses and design of supporting structures

Dr Ali Saleh, Mr Christopher Keonig and Ms Yukari Aoki for Finite Element Analyses

Mr Peter Brown and Mr Rami Haddad for overseeing and conducting push over and shake table tests

Mr Vitali Bebekh for analyses of test data

Mr Berkay Dincel for testing and analyses of flexural members

Mr Laurence Stonnard and the staff of UTS Engineering Workshop, Concrete Laboratory and the Structures Laboratory for the fabrication of test specimens and supporting structures

Executive Summary

At the request of Dincel Construction Systems Pty Ltd, the specialist consultants at accessUTS were engaged to test and analyse the adequacy of Dincel-Wall for installation in seismic regions. accessUTS is a division of the University of Technology Sydney in Australia which provides specialist consultancy services to the Australian industry. The testing and analysis program was designed and completed over a period of 20 months.

The experimental program consisted of fabricating two large wall specimens (2.8m high by 3.0m wide) namely "A" and "B" using the Dincel system. The specimen "A" was centrally reinforced and specimen "B" reinforced with minor reinforcement only as shown on the drawings at Appendix A at the end of this report. The specimen "B" with minor corner reinforcement is referred to as unreinforced wall specimen hereinafter. After curing, the unreinforced wall specimen "B" was initially tested on the UTS shake table facility using the strong ground motion record of Kobe earthquake of 1995 (Figure 2.1) and El Centro, California earthquake of 1940 (Figure 2.2) as input, representing large magnitude near field and far field earthquakes, respectively. The shake table tests clearly confirmed the strength of the unreinforced wall specimen "B" in withstanding typical large magnitude earthquakes.

However, due to the much larger relative stiffness of these wall specimens compared to those used in multi-storey buildings as part of the shear wall system, the resulting inter-storey drifts were well below those demanded by large earthquakes and hence it was decided to subject these walls to push over tests to confirm their adequacy in providing the required displacement demand of 5.3 mm arrived at by Finite element analysis of a typical 7 storey concrete building with shear walls as its lateral load resisting system.

The two walls were placed side by side on the strong floor of the Structures Laboratory at UTS and pushed sideways by two 100 tonne jacks, reacting against

each other. The jacks provided "in-plane" loading conditions to simulate earthquake forces to be resisted by shear walls in buildings. The tests confirmed that the walls, even the unreinforced wall specimen "B" has adequate capacity to accommodate the displacement demand imposed by large earthquakes within the elastic range.

Finete Element (FE) modelling for a conventional concrete 'U' shaped wall similar to Sample 'B' of the push over test was carried out. A lateral load as per the push over test was applied at the top of the FE wall model and lateral deflections determined. These deflections were then compared with the lateral deflection measurements of Sample 'B' of the push over test. The comparisons of the results conclude that **"both plain concrete and Dincel Wall have similar lateral stiffness and that the polymer encapsulation of Dincel Wall does not reduce the lateral stiffness of the system"**.

It is known that short stocky buildings, around 6 to 10 storeys in height, display more damage during an earthquake event than buildings that are of greater height. The supporting analytical computer finite element studies on a typical seven storey building subjected to the 1995 Kobe and 1940 El-Centro earthquakes have confirmed that the stresses at the base of the walls can be kept below typical compressive strength of concrete walls (namely, around 32 MPa) provided approximately 12 meters of walls are provided along each axis of the building for the more severe Kobe earthquake. For the smaller magnitude El-Centro earthquake, the required wall length is smaller. The analyses also reveal that the maximum inter-storey drift demand is around 5.3mm for Kobe earthquake in order not to exceed the assumed compressive strength of concrete of 32 MPa. Clearly, if higher strength concrete is used, the length of walls to accommodate seismic forces can be less than 12 meters and should be determined through rational analysis and design by the responsible engineer. The push over tests confirmed the ability of the walls to sustain the required displacement of 5.3 mm, but this does not mean a conventional concrete wall with adequate steel reinforcement cannot accommodate the same displacement demand. Therefore, there was a need to establish the strength of the Dincel Wall in

DINCEL
STRUCTURAL WALLING

the post elastic range and its superior ductility, offered by resilient Dincel Polymer encapsulation.

To address this issue, and in consultation with Dincel engineers, it was decided to fabricate, analyse and test two flexible specimens and subject them to severe shaking near resonance conditions. The specimens were of identical sizes, 4m high, 640mm wide and 195mm thick. One specimen was fabricated using the Dincel system called specimen "C" and the other one using reinforced concrete as a conventional system called specimen "D". Both systems were reinforced at the centre of the wall for exact comparisons with 1 x 16Ø bar at 350mm centres (i.e. 2 x 16Ø bars for each 640mm wide sample) as shown in Appendix A at the end of this report. These 2 x 16Ø bars at the centre of each sample "C" and "D" were placed for the purpose of safety in the event that premature failure occurs during the shaking of the samples thus preventing damage to the earthquake shake table as well as assisting lifting of the samples onto the shake table. The position of steel bars at the centre of the samples represents no important flexural strength to samples being shaken in the weak axis direction to resonance conditions. Therefore samples "C" and "D" are deemed as unreinforced samples as tested in the out of plane direction. The main objective of this exercise was to establish and directly compare the resilience of the Dincel wall with that of the conventional wall in sustaining large deformations, well in excess of what the codes allow. To achieve large deformations, it was therefore necessary to expose the specimens to out of plane loads on the UTS shake table at or near resonance conditions.

From these tests on samples "C" and "D" it was observed that the Dincel system could undergo maximum deformations of up to 145 mm (145/3300 = 4.4%) which is well in excess of collapse performance level of table 5.1 and despite having internal cracking, the Dincel system sample "C" was able to carry the load safely at 4.4% displacement level. Such large displacements are likely to occur for earthquakes registering magnitude of 8.5 and above on the Richter scale. On the other hand, the maximum safe displacement for the system made up of traditional concrete as per sample "D" was only 70 mm, less than half of that of the Dincel system.

A ratio of more than 2 to 1 in accommodating large displacement is a testimony to Dincel Walls' superiority as an effective aseismic system.

An obvious advantage of the Dincel Wall system is the provision of sound confinement to the concrete by the cellular polymer encapsulation which incorporates the outer skin as well as the integral internal webs (refer Figure 1.2). Such a system will prevent the deterioration of stiffness and possible collapse by not allowing the concrete to spall after several loading cycles even if fully cracked. The tests with unreinforced wall specimen "B" was not cracked when the push over test was terminated. The test with specimen "C" Dincel sample displayed cracks at the deformation level of 4.4% (145mm).

Even at this displacement level Dincel sample "C" was deemed as safe in terms of possible threat to human life, clearly demonstrating the advantage of using Dincel Wall for additional safety where large displacements demands are required for a safe aseismic design. This is a welcomed safety feature for walls subjected to strong ground motions.

These tests proved to be very conclusive in demonstrating the capacity of unreinforced Dincel system in sustaining larger deformations caused by major earthquakes of magnitude of 8.5 and over on the Richter scale.

In addition to testing wall systems, a complementary study also confirmed the superiority of Dincel system used as flexural members over beams made of traditional reinforced concrete, in terms of larger load carrying capacity and much improved ductility.

The tests to date have displayed excellent capacity of all Dincel Wall samples. For a number of reasons including earthquake after shocks, fire, explosions, e.g. gas, the earthquake resisting shear walls, especially for post-cracking state are required to be reinforced as per specimen "A" as shown on the drawing at the end of this report.

DINCEL
STRUCTURAL WALLING

The non-earthquake resisting Dincel Walls, i.e. walls designed primarily for vertical gravity loads can be unreinforced subject to the top and bottom of the wall being positively connected to the footings/slabs as shown on Figure A.1 at Appendix A. This will be true since the capacity of the unreinforced Dincel specimen was tested to be adequate even for earthquake magnitude of 8.5 and above. **Therefore, the designer may choose to reinforce an adequate length of the Dincel Wall for earthquake shear wall purposes only and the remaining walls can be left unreinforced.** This way prevention of collapse of the unreinforced walls during an earthquake event is provided by polymer encapsulation of the unreinforced concrete wall and the positive connection at the top and bottom of the walls as shown on Figure A.1 at Appendix A.

The conventional concrete structures are considered to be in the collapse range when displacement levels exceed 2.5% (refer Table 5.1). The tests demonstrated that Dincel sample 'C' safely withstood 4.4% displacement level.

This performance level will be particularly important to strengthen existing buildings and building structures which require post disaster functioning. This performance is not achievable with conventional materials when displacement levels exceed 2.5%.

Based on the above, when an adequate length of Dincel Wall, reinforced as a shear wall as per specimen"A" shown at the end of this report is provided, the Dincel Wall is capable of addressing the structural safety required to protect human life in damaging earthquakes with magnitude up to 9.0 on the Richter scale.

1 Introduction

1.1 Dincel Construction System

Dincel Construction System is an innovative method of constructing load bearing concrete walls. The system consists of a rigid and durable polymer that is used as permanent formwork which encases ready mixed concrete. The permanent polymer formwork is manufactured under factory conditions and arrives on site in large modules. The modules are sized specifically for each job and are joined together using waterproof 'snap together' joints, enabling large wall elements to be constructed to match any building layout.
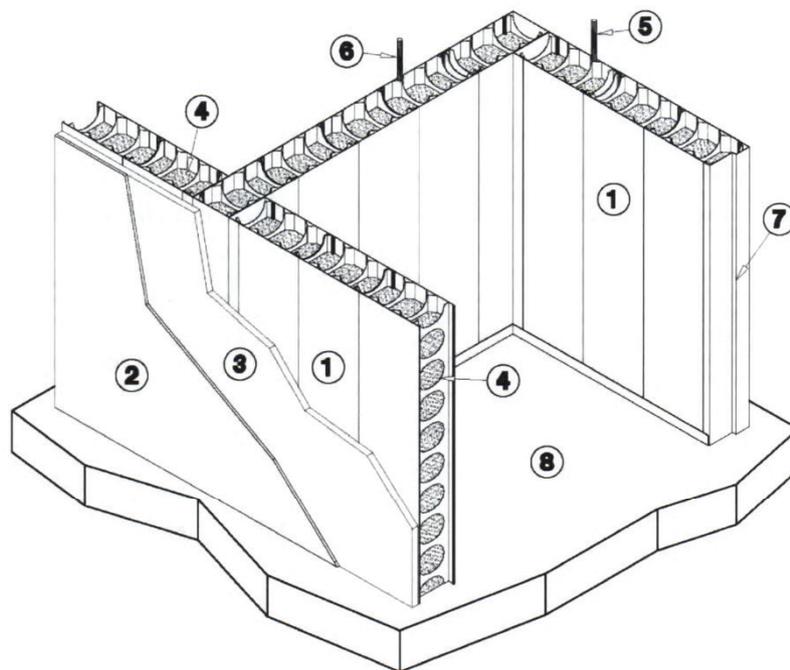
① DINCEL-WALL
② Acrylic render/plasterboard finish insulation (optional)
③ Insulation (optional)
④ Concrete
⑤ Service Space/electrical, communication cables
⑥ Service Space/water pipes
⑦ Door Jamb
⑧ Floor

Fig 1.1 – Dincel Construction System (Dincel Construction Manual 2011)

The Dincel Construction System provides a cost effective alternative to conventional concrete walls, as it reduces construction time and the amount of skilled labour which would be required to erect and subsequently strip conventional timber formwork. The permanent polymer of Dincel Construction System also has the advantage of increasing the fire resistance, durability, and water proofing of concrete walls.

The external polymer walls are connected together by a polymer 'web' system which provides stability to the individual modules before the concrete is poured and also enables the inclusion of steel reinforcement. The 'web' consists of circular voids which are specifically aligned to enable the steel reinforcement to be placed inside the wall in a systematic grid pattern. However, the internal polymer 'web' does not provide enough room for a vibrator to adequately aerate and compact the concrete. The polymer 'web' and its circular voids are clearly illustrated in Figures 1.1 and 1.2.
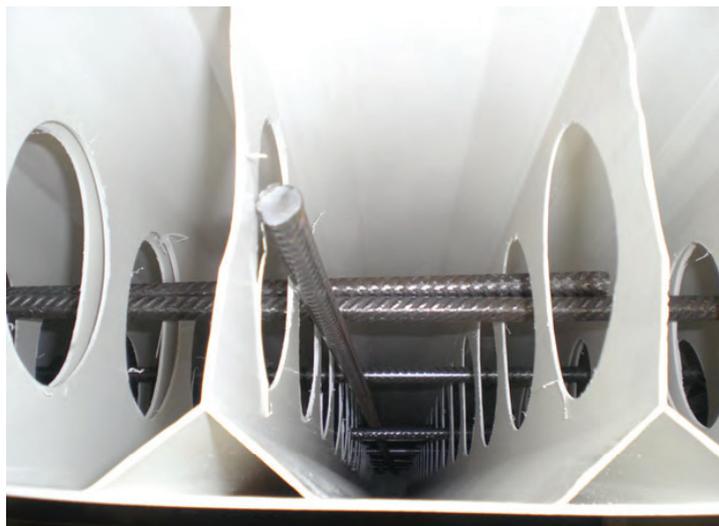
Fig 1.2 – Internal polymer 'web'

1.2 Scope of the work

The scope of the work as part of this project includes the following:

- Analytical Studies
- Experimental Studies

For both studies two types of structural systems were considered, namely, a U-shapes wall specimen with shear wall dimensions of 2.8m (height) and 3.00 m (width) loaded in-plane, acting as a shear wall with two out-of-plane wings; and a narrow high wall with large height to width aspect ratio behaving more like a blade column and loaded along its weak axis. For both specimens the thickness of the walls were 195 mm which is the thickness of Dincel concrete infill excluding Dincel polymer encapsulation.

The main objective of these studies were to
- Demonstrate the suitability and adequacy of Dincel system as a promising shear wall system for seismic applications in highly seismic regions of the world
- Demonstrate the superiority of the Dincel system over conventional systems in undergoing large deformations without the risk of failure or collapse.

The findings of this study confirm both above-mentioned objectives.

2   Analytical Studies

To guide and inform the experimental studies, some detailed analytical studies were required to determine the anticipated response of a typical mid-rise building with Dincel walls, as its main lateral load resisting system, subjected to severe earthquake loads.

For the U-shaped wall system a detailed Finite Element model of the entire building was developed and analysed. For the narrow high wall, a simple Finite Element model, verified by the closed form solution of a simple cantilever was utilised. For both systems the Kobe earthquake of 1995 with Peak Ground Acceleration (PGA) of 0.83g and magnitude of 7.3 on the Richter scale (representing a near field earthquake – see Fig. 2.1)) and the El-Centro earthquake of 1940 with a PGA of 0.35g and magnitude of 7.1 on the Richter scale (representing a far field earthquake - see Fig 2.2) were used as the design earthquakes representing severe and destructive ground motions.

DINCEL
STRUCTURAL WALLING
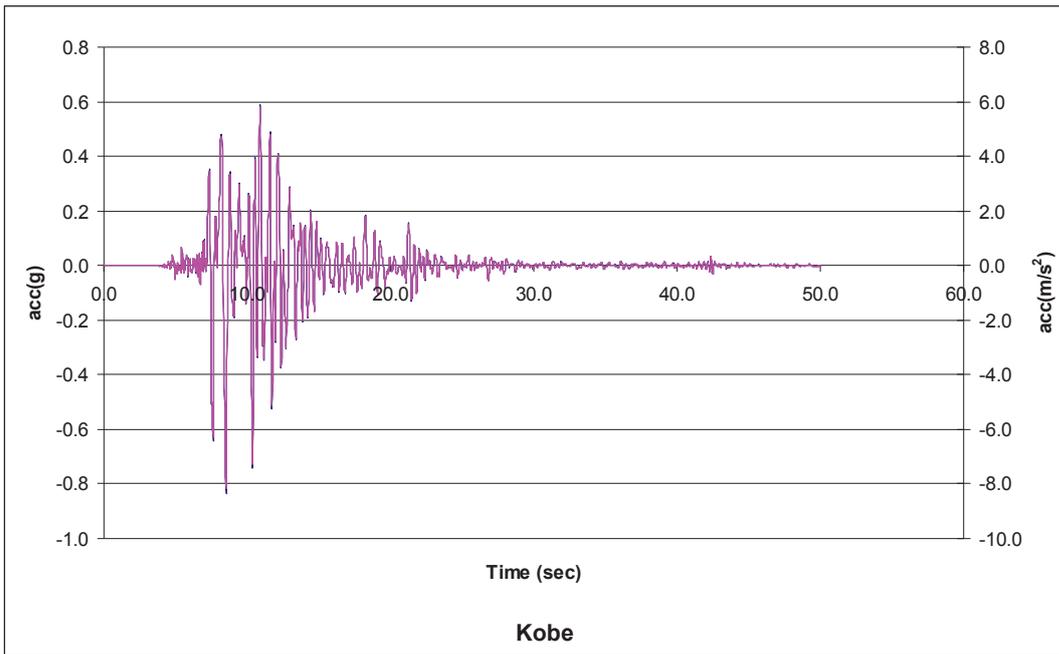
Fig 2.1 – Acceleration Time History of 1995 Kobe earthquake with Peak Ground Acceleration of 0.83 g registering 7.3 magnitude
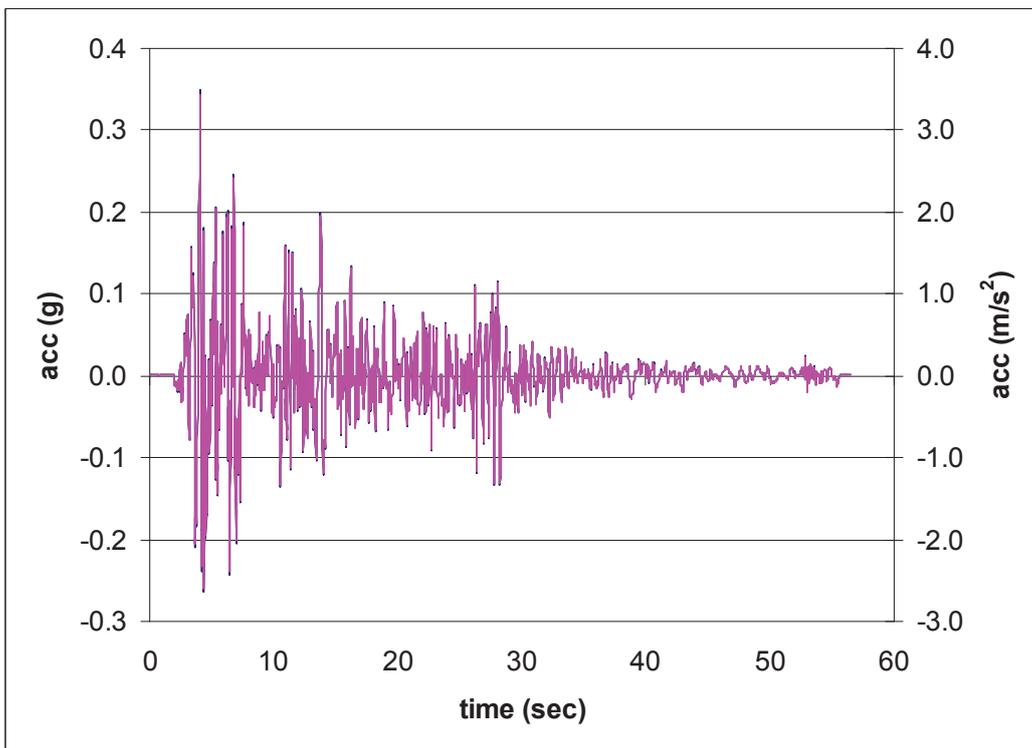
Fig 2.2 – Acceleration Time History of 1940 El-Centro earthquake with Peak Ground Acceleration of 0.35 g registering 7.1 magnitude

3 Modelling of the Building and Push Over Test Panel

3.1 Geometry of the Building

It is known that short stocky buildings, around 6 to 10 storeys in height, display more damage during an earthquake event than buildings that are of greater height. Therefore, to simulate the response of Dincel Walls to such earthquakes in a typical short stocky building structure, a seven storey building with concrete slab, perimeter columns and lift cores made up of Dincel wall system were modelled using Finite Element (FE) modelling and analysis. The structural concrete components of each level are set-out in an open rectangular arrangement as shown in Figure 3.1 below, comprising of uniform slabs rigidly connected to supporting columns and lift core walls, in what is called a flat plate structure.
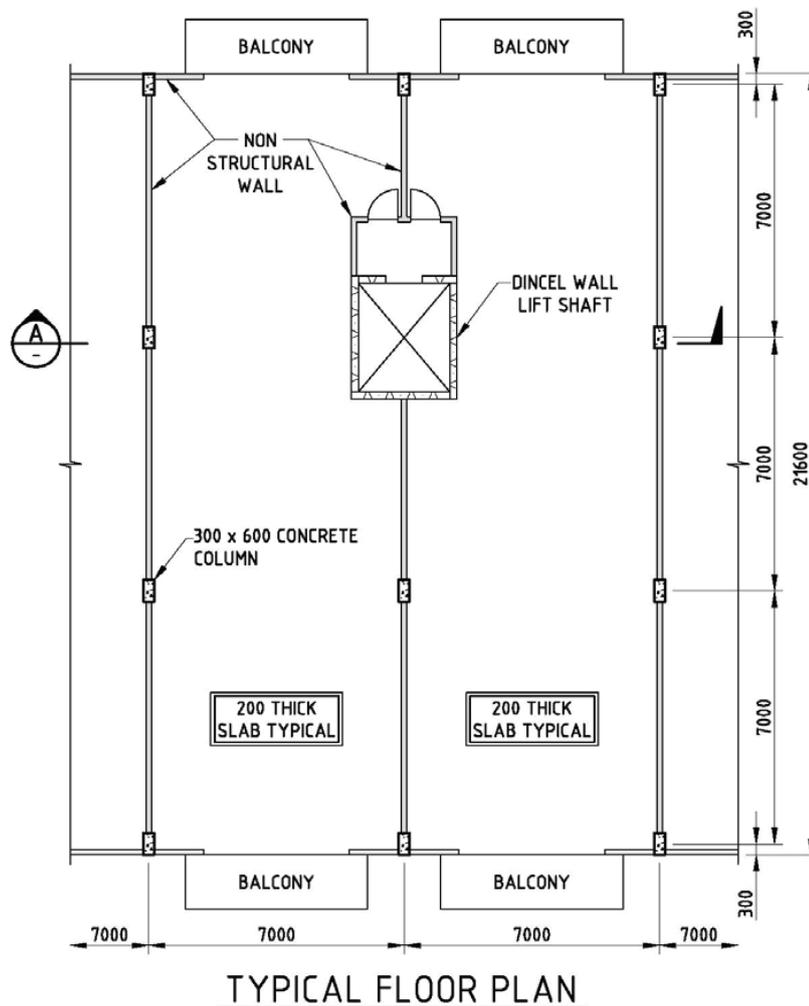
TYPICAL FLOOR PLAN

Fig 3.1 – Typical Floor Elevation
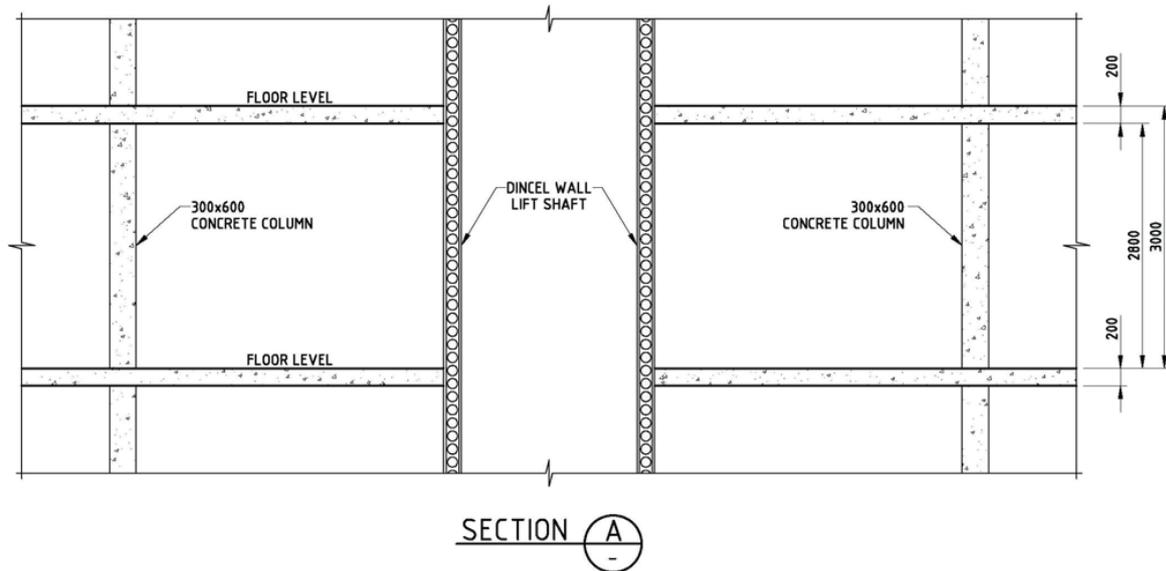
Fig 3.2 – Building Section

Fig. 3.2 above shows a typical floor-to-floor height of 3.0m. It also indicates that the columns extend the full height of the building with constant cross section dimensions of 600 x 300 mm. Similarly, the Dincel lift core walls also extend the full height of the building with a constant thickness of 200mm. Each slab has a uniform thickness throughout each level. Levels 1 to 6 are 200mm thick while the roof has a thickness of 235mm to allow for drainage falls.

3.2 Material Properties and Gravity Loading

The material properties of the concrete used in this building, and the applied gravity loading which is specific to the overall function of the building, are listed in Tables 3.1 and 3.2, respectively. These parameters are explicitly defined in the pre-processing stage of the modelling process, and have a significant contribution to the structural behaviour of the building. Table 3.1 summarises the applied loading by separating the permanent loads (dead loads) and imposed loads (live loads).

Table 3. 1– Summary of Applied Loading

	Dead Load		Live Load
	Densities t/m^3	SDL kpa	kpa
L1 - L6	2.548	1.5	2.0
Roof	2.548	1.5	3.0
Columns	2.548	N/A	N/A
Lift Core	2.184	N/A	N/A

The self weight of the building is defined by the density of the concrete. It should be noted that the Dincel lift core has a lower density than the conventional concrete. The lower density accounts for the volume of concrete which is excluded from the walls to include the internal polymer 'web' of the Dincel Construction System.

The following concrete material properties were used:

Table 3.2 – Summary of Defined Material Properties

Element	Young's Modulus (Pa)	Concrete Strength MPa	Poisson's ratio
Lift Core, columns and slabs	3.23×10^{10}	32	0.2

3.3 Finite Element Model of the Building
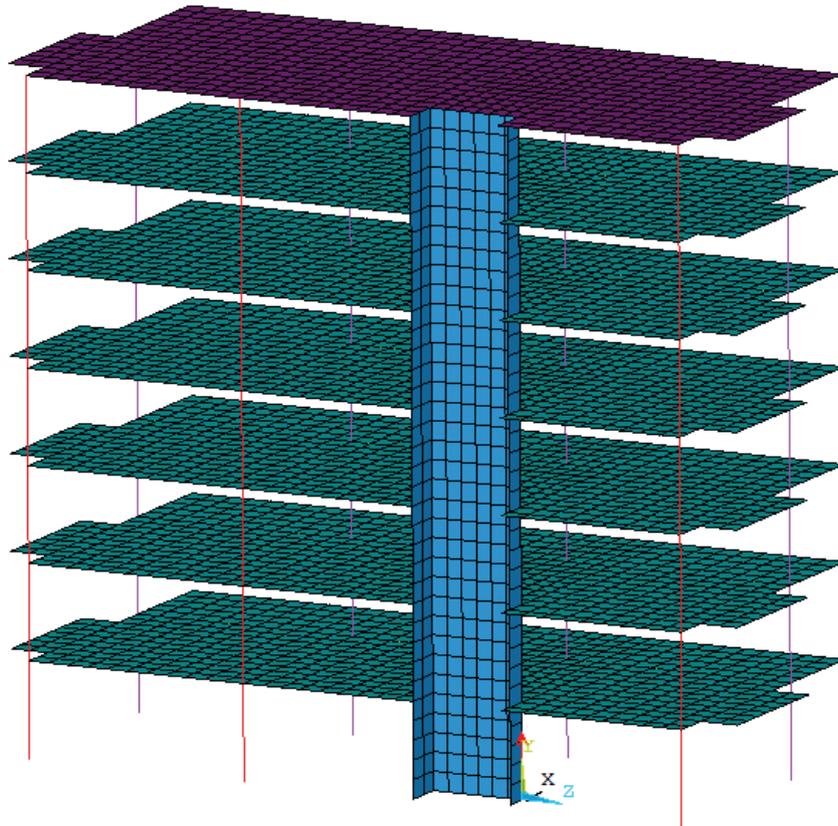
Fig 3.3 – Model of the Entire Building
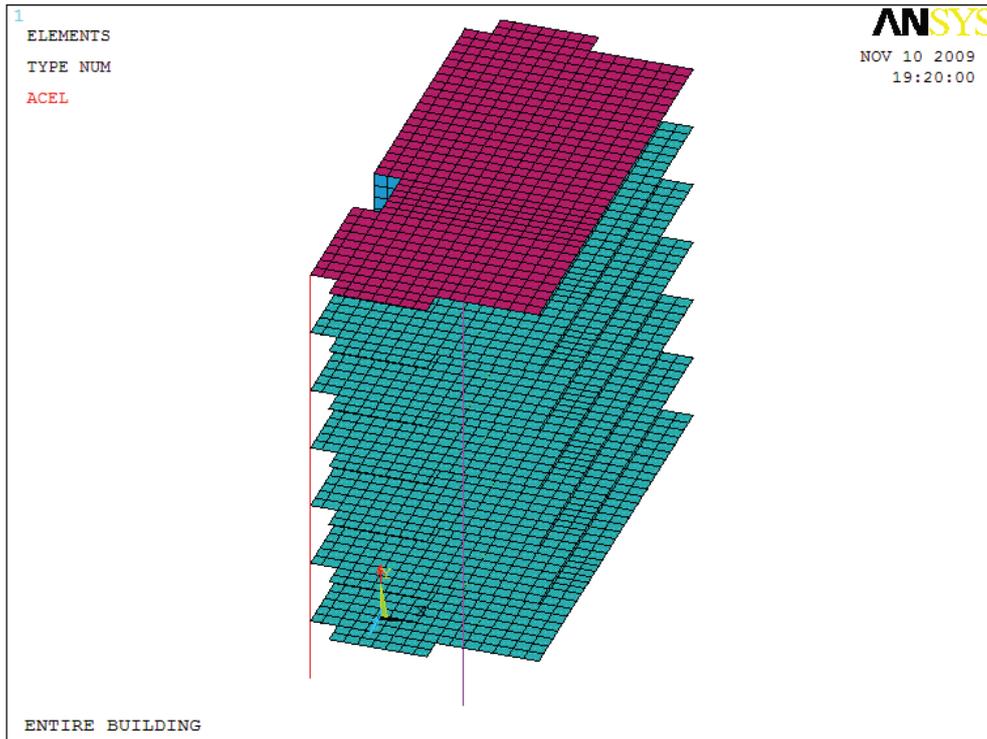
Fig 3.4 – Model of the Entire Building (another view)

Figures 3.3 and 3.4 show the 7 storey building modelled using ANSYS analysis software. Advantage was taken of the symmetry of the building along both horizontal axes in an effort to minimise the size of the model, and this is can seen in Figures 3.3 and 3.4 as only half of the slab layout and lift core are shown. The Beam4 finite elements used to model the columns, and the Shell93 elements used to model the lift core and slabs can clearly be seen. The different colours in Figures 3.3 and 3.4 represent elements which were assigned different material and geometric properties. Due to the reflective symmetry, only half the cross sectional dimensions of the columns along the symmetry line were required to be modelled and they are represented by the red column elements.

The square shell elements used to model the floors are illustrated in Figure 3.5.
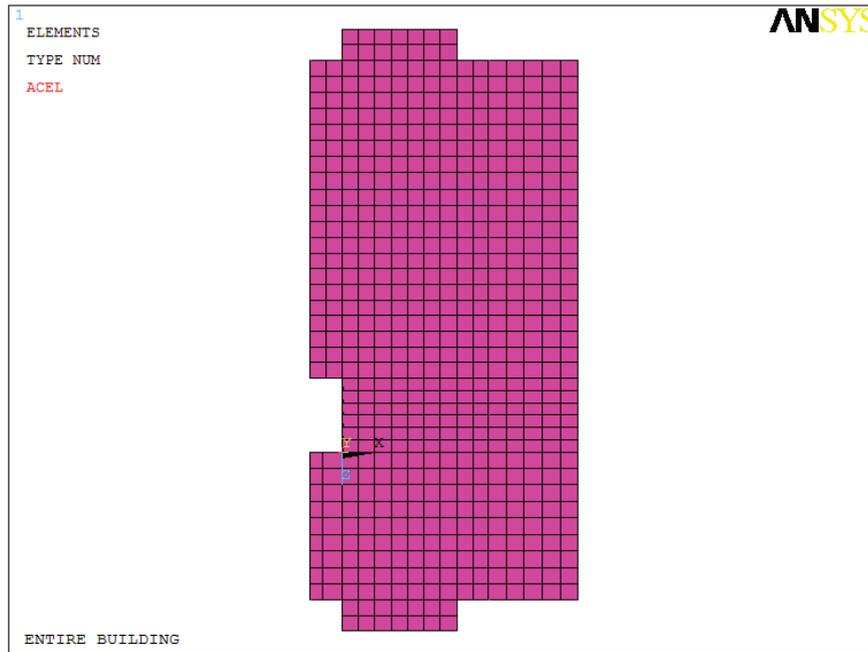
Fig 3.5 – Plan View of a Typical Floor Modelled in ANSYS

3.4 Model of Lift Core Segment
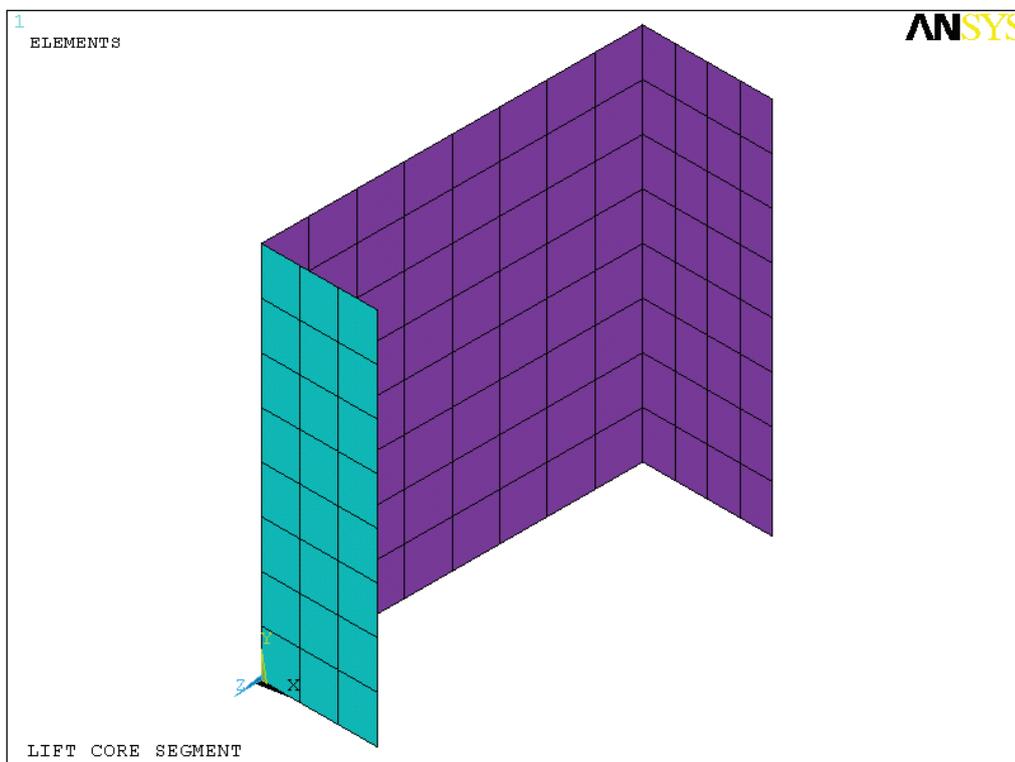
Fig 3.6 – Model of Lift Core Segment

Figure 3.6 shows the model of the lift core segment. The lift core segment is 2,800 mm tall, equal to one storey of the entire building. Fixed support conditions were modelled at the base of the structure while the top of the structure is left unsupported. Symmetry could not be used to reduce size of the model because the 2 wing walls are not the same length. Shell93 element was selected from the ANSYS library to model the structure.

3.5 Finite Element Analysis of the Building

Given that Kobe earthquake was the bigger of the two earthquakes, the dynamic response of the building subjected to only Kobe earthquake is covered in this section, knowing that the results for El-Centro earthquake were less severe and hence not as critical.

A transient dynamic analysis was performed on the model of the 7 storey building using a typical amount of damping for the purpose of the analysis.

The response covering the period from the 6th to the 13th second is presented here. This 7 second duration captures the most intense period of the earthquake (refer to Figure 2.1) resulting in maximum response effects and producing the most severe stresses and displacements in the lift core.

3.6 Results of Analyses

Displacements and Deflected Shape

Figure 3.7 shows that the Kobe earthquake displaces the base of the building by a maximum of 350 mm. The same figure shows the maximum acceleration of 0.83g as referred to earlier.
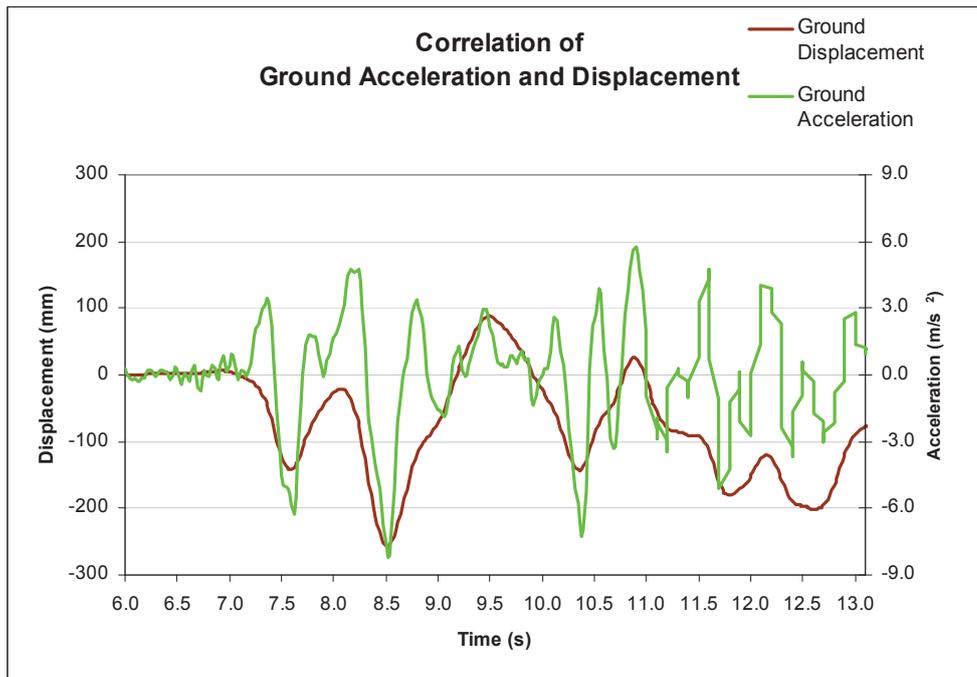
Fig 3.7 – Correlation of Ground Acceleration and Displacement of Building

Figure 3.8 displays a time history plot of the longitudinal displacement of the lift core at each level of the building. The displacements at each level are calculated relative to the ground displacement. Figure 3.8 illustrates that the higher levels have a greater displacement than the lower levels, as expected.

Figure 3.8 also identifies that the maximum displacement relative to the ground displacement occurs after 8.76 seconds of excitation and has a maximum value of 141.5 mm at the roof. The roof is 21m above the ground and therefore this displacement equates to SPAN/150 in engineering terms. Although this level of displacement is within the limits acceptable by most earthquake codes, the resulting normal concrete stress at the base of the building will far exceed the 32 MPa strength assumed for the core wall. Based on this finding the building was reanalysed using more wall modules as will be seen later.

Figure 3.9 displays a plot of the inter-storey displacement (or drift) at each level of the lift core. It illustrates that the inter-storey displacement of the lower levels of the building are again smaller than that of the upper levels. This figure also identifies

DINCEL
STRUCTURAL WALLING

that the maximum inter-storey displacement occurs after 8.76 seconds and is equal to 25.1mm. Unlike the displacement relative to the ground, the maximum inter-storey displacement is found to be at level 6.
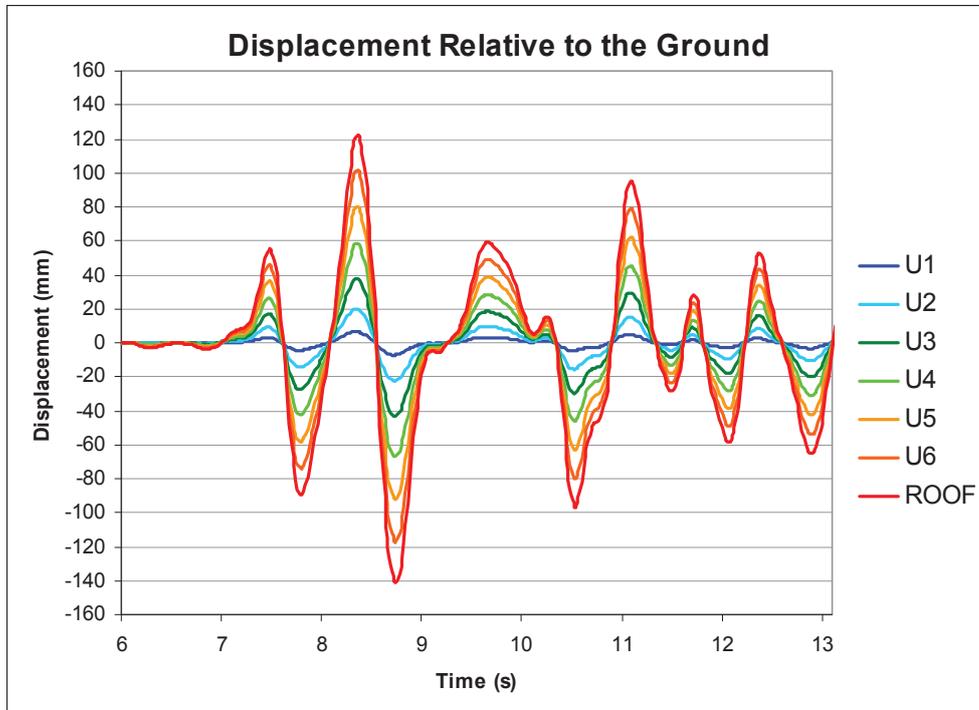
Fig 3.8 – Displacement of Building Relative to Ground
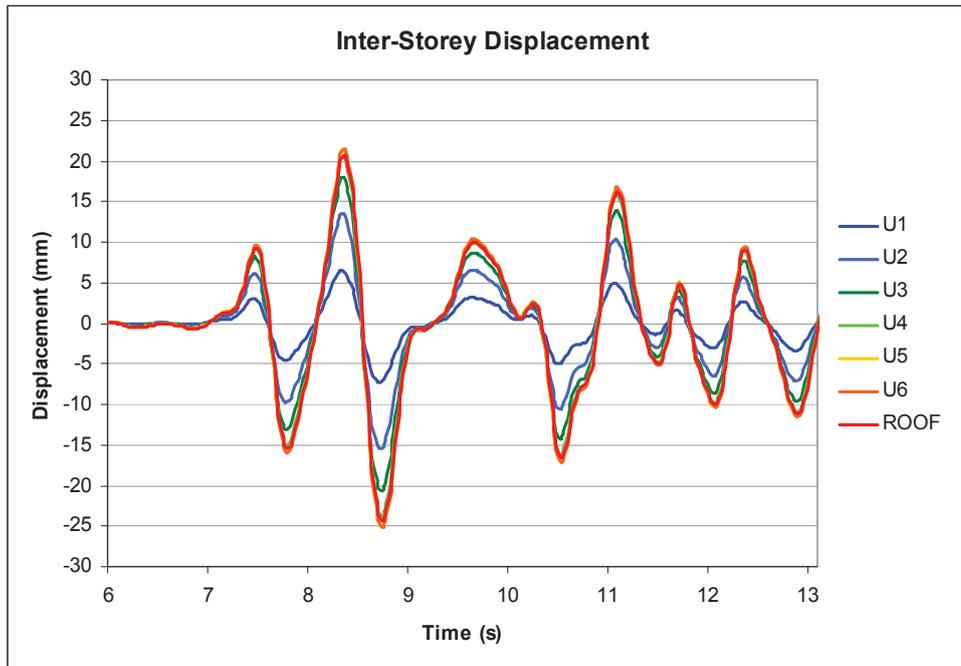
Fig 3.9 – Inter-Storey Displacement at Each Level

The distance between each line of Figure 3.9 represents the rate of change in the displaced shape of the lift core, and this can be interpreted as the curvature of the lift core. A greater distance between adjacent lines indicates a greater curvature of the lift cores deflected shape. Therefore, Figure 3.9 indicates that the curvature is greatest at the base of the lift core, and shows a decreasing trend until level 4, where the remaining levels are experiencing similar inter-storey displacement and are therefore deflecting in a relatively linear fashion. However, due to the fact that the inter-storey displacement of the roof level is less than level 6, this suggests that the very top of the structure is beginning to experience reverse curvature.

In Figures 3.10 to 3.16 the first seven mode shapes of the building are displaced. From these figures it is clear that the first two modes are global modes corresponding to first and second modes of the core while modes 3 to 7 are local modes associated with deflection of the floors. Therefore only the first two modes are crucial in any subsequent analyses.
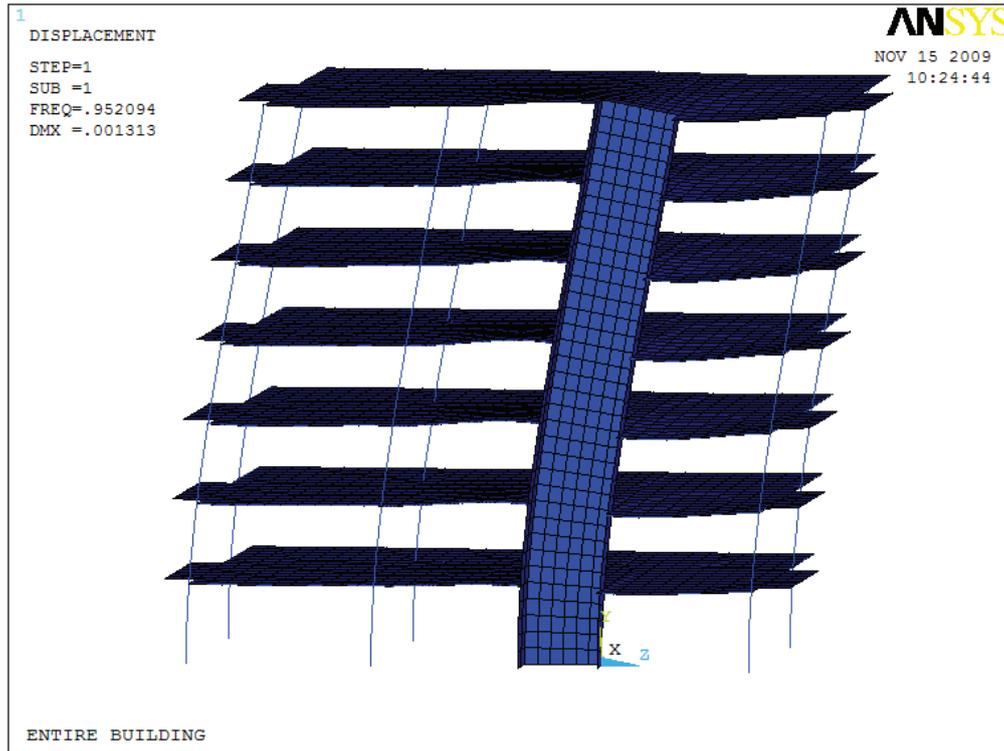
Fig 3.10 – 1st Mode Shape of the Building
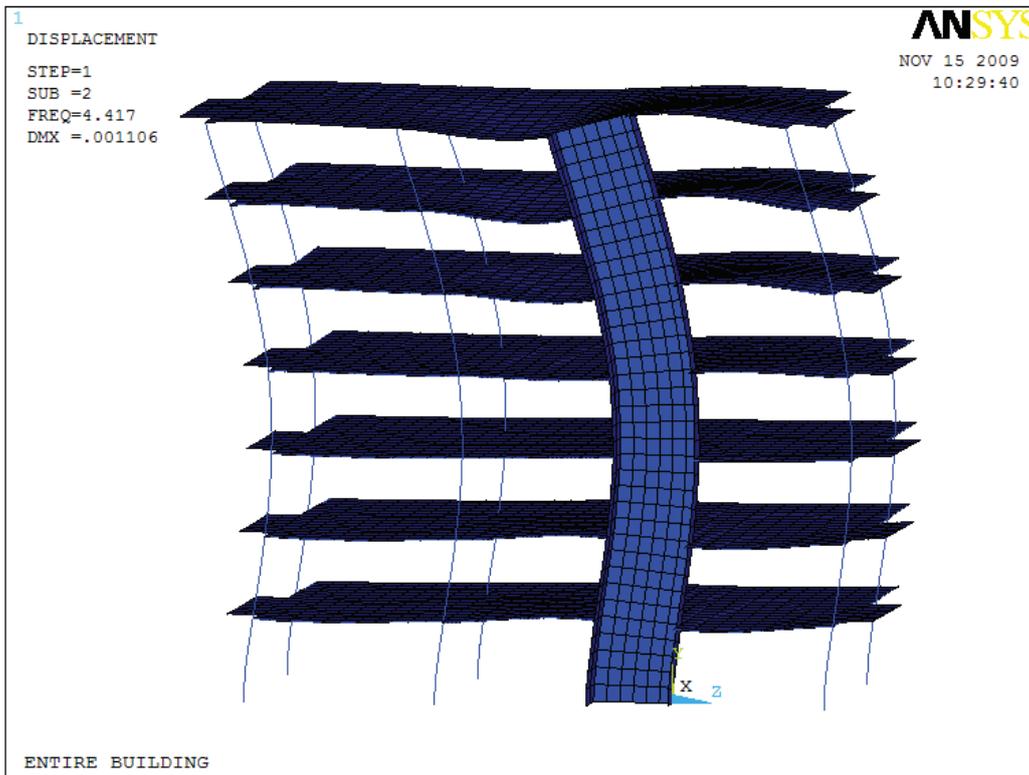
Fig 3.11 – 2nd Mode Shape of the Building
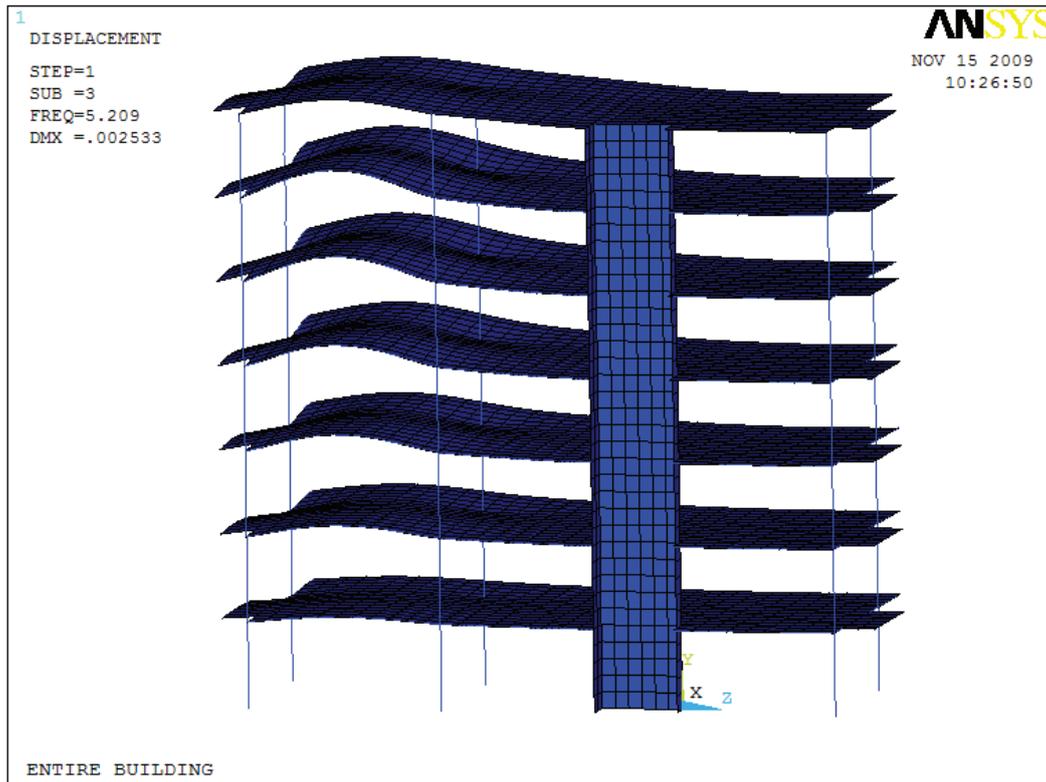
Fig 3.12 – 3rd Mode Shape of the Building
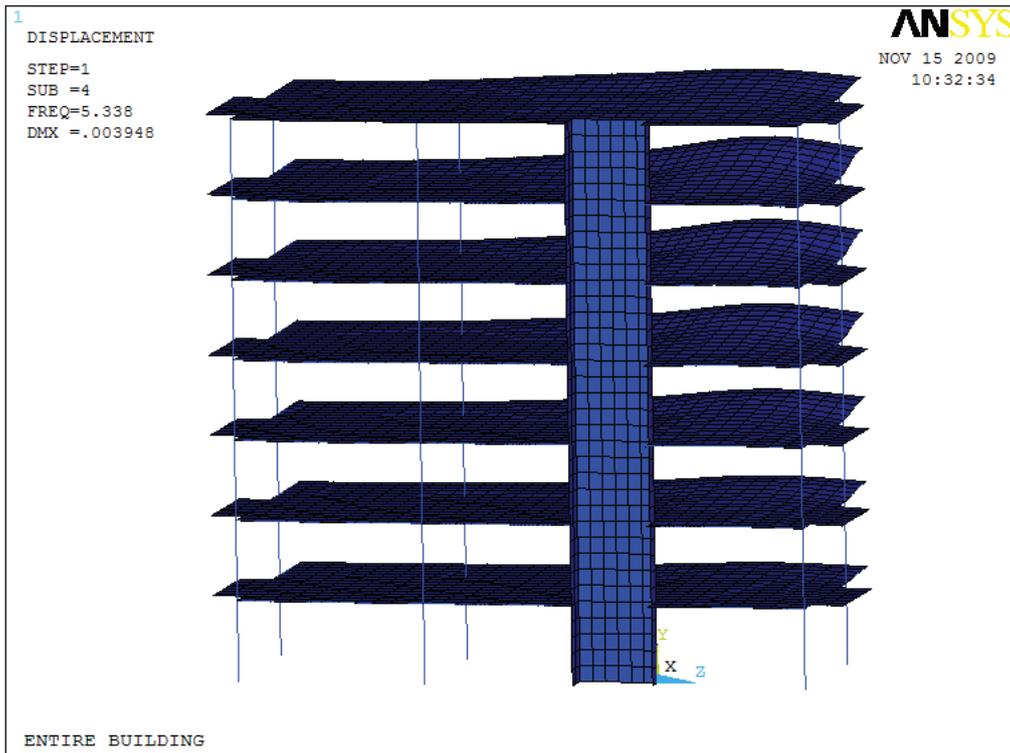
Fig 3.13 (a) – 4th Mode Shape of the Building (view 1)
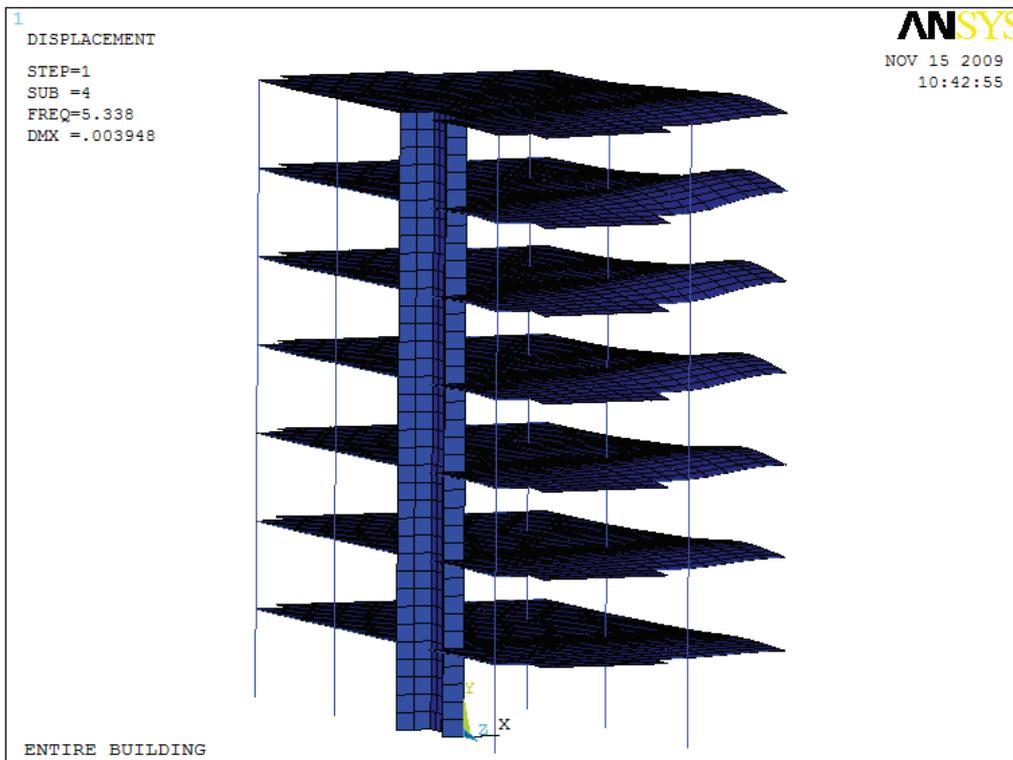
Fig 3.13 (b) – 4th Mode Shape of the Building (view 2)
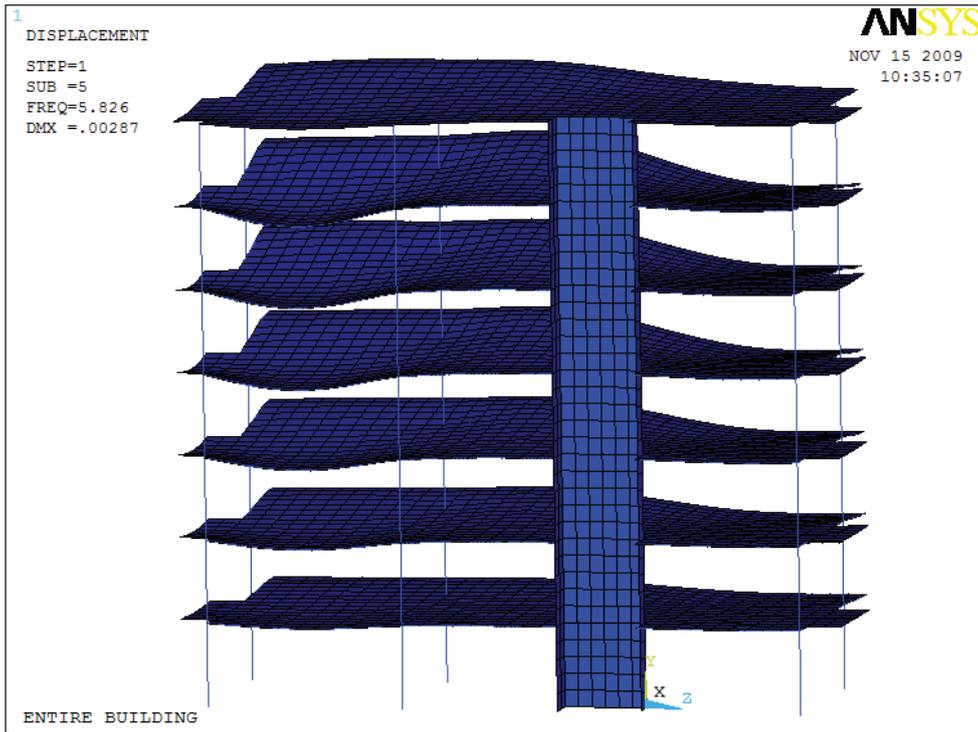
Fig 3.14 (a) – 5th Mode Shape of the Building (view 1)
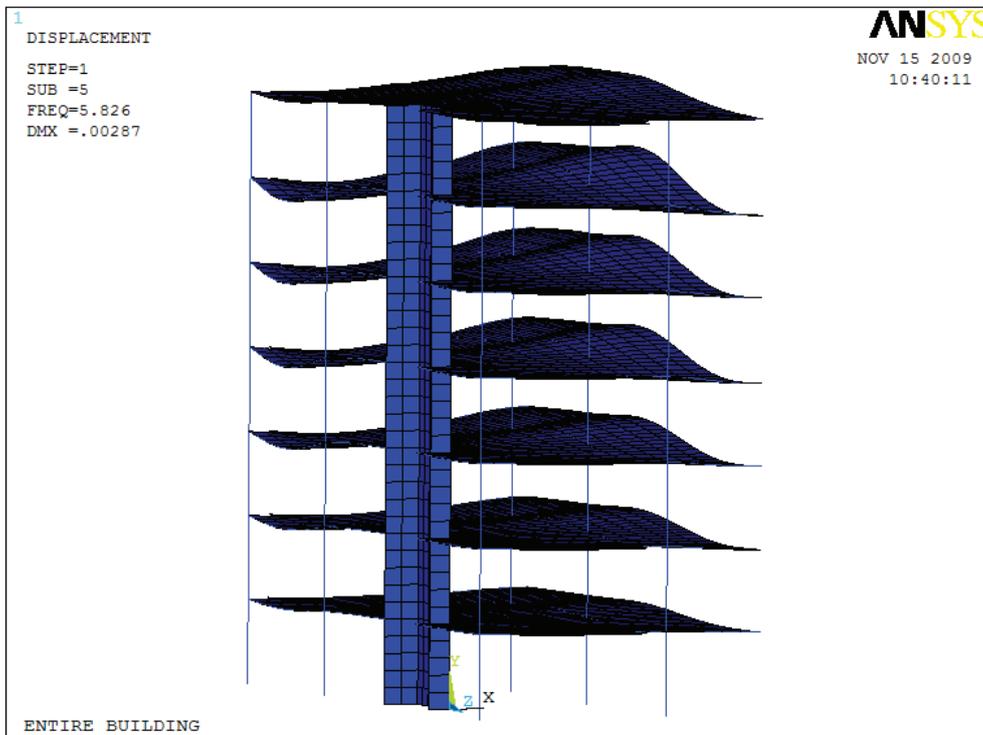
Fig 3.14 (b) – 5th Mode Shape of the Building (view 2)
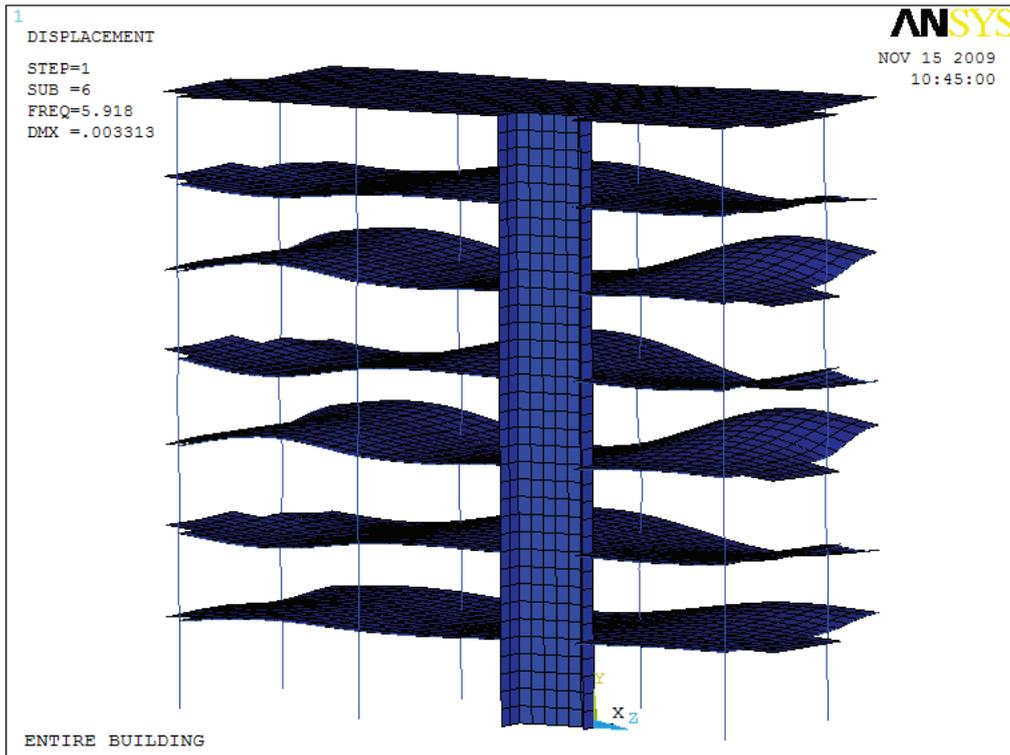
Fig 3.15 (a) – 6th Mode Shape of the Building (view 1)
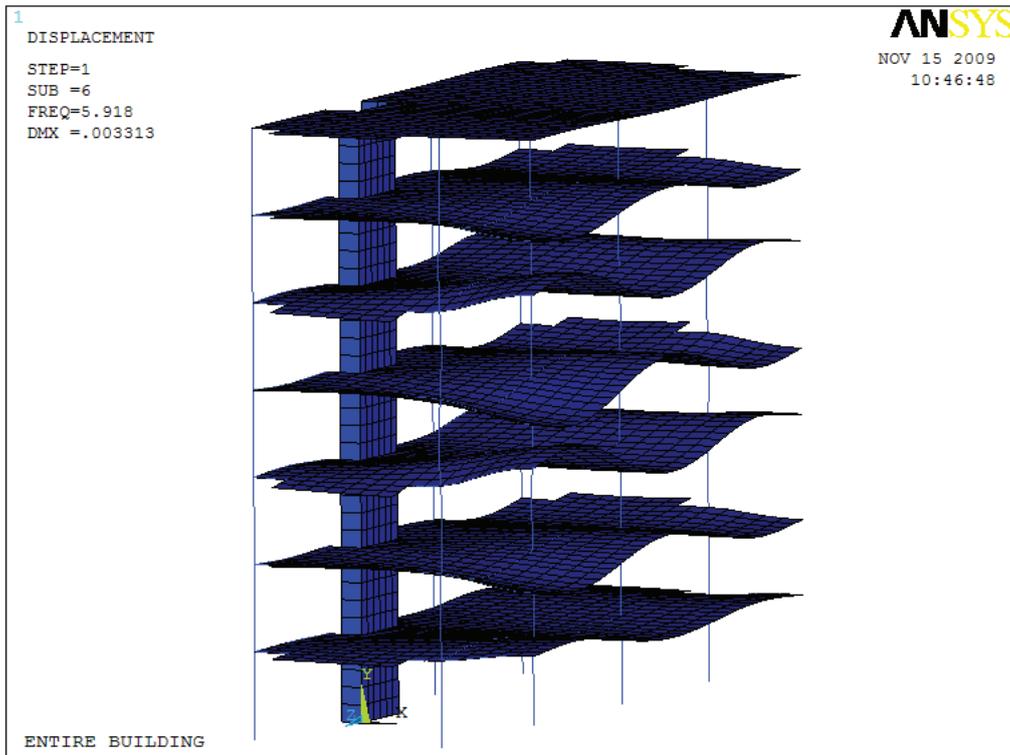
Fig 3.15 (b) – 6th Mode Shape of the Building (view 2)
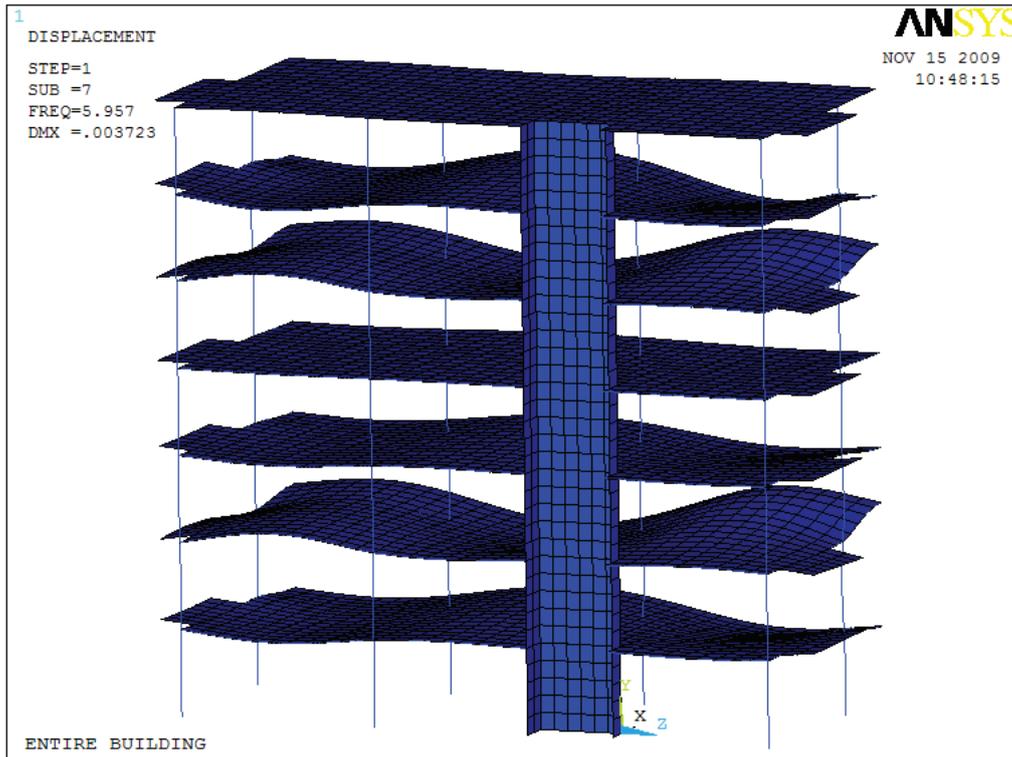
Fig 3.16 – 7th Mode Shape of the Building

The corresponding natural frequencies of the analysed building are given in Table 3.3 for the first 5 modes.

Table 3.3 – Natural frequencies of the building obtained from FE analysis

mode	Hz
1st	0.95
2nd	4.42
3rd	5.21
4th	5.34
5th	5.83

Reactions at the Base of the Building

Table 3.4 shows the total reactions at the base of the building when it is subjected to the forces imposed by the most severe point in the duration of the earthquake (8.76 seconds).

Table 3.4– Summary of Reactions at the Base of the Building

	Lift Core		Columns		Total	
	Force (kN)	%	Force (kN)	%	Force (kN)	%
Longitudinal Reaction (z)	2824	94%	180	6%	3004	100%
Transverse Reaction (x)	769	99%	7	1%	776	100%
Vertical Reaction (y)	3043	18%	13413	82%	16456	100%

This table supports the expectation that the 'shear wall system' (Lift Core) is the primary source of lateral stiffness in the building, whereas the 'flat-plate system' is secondary. Interestingly, Table 3.4 clearly indicates that the lift core is by far the primary source of lateral stability as it attracts 94% of the lateral forces as apposed to the 6% attracted by the columns. This clearly indicates the importance of understanding how the lift core responds to dynamic loads.

Stresses in the Lift Core

Both the normal stresses and shear stresses in each of their 3 directions, and also the resultant Von-Mises stress, were extracted from the model. A summary of the maximum stresses in the lift core can be found in the following Section. The locations of the maximum stresses are generally where the lift core connects to the ground or to the suspended slabs.

Figures 3.17 and 3.18 illustrate the flexural stresses throughout the lift core, which are also labelled as vertical stress in the y-direction. Both figures show that the maximum stresses are located in the wing walls of the lift core which are behaving in a similar fashion as the flanges of a square hollow section. Figure 3.18 focuses on the base of the lift core where the maximum stresses are situated and illustrates that the most critical point is located at the corner where the 2 lift core walls meet and connect to the ground. This maximum stress has a value of 81.80 MPa which well exceeds the concrete strength of 32 MPa used in the lift core and will therefore result in cracking of the concrete. However, as will be shown later, as part of the shake table tests, a cracked concrete in a Dincel wall can still accommodate the large displacement demands of a major earthquake without failing due to confining effects of the polymer encapsulation which proved to be instrumental for a safe system. Nevertheless, to complete the analysis for the sake of comparison with conventional

DINCEL
STRUCTURAL WALLING

systems, the FE analysis was repeated using four wall modules rather than one in order to reduce the maximum flexural stress to below 32 MPa which lead to a much stiffer system with smaller overall displacements and much smaller inter-storey drifts as will be reported later.

3.7   Summary of Results

The results of the FE analysis for the 7 storey building with a single wall unit can be summarised as follows:

Maximum Displacements:

- Maximum Displacement Relative to Ground = 141.5 mm
- Maximum Inter-Storey Displacement = 25.1 mm

Maximum Stresses in the lift core at the time of maximum displacements:
- Normal Stress in the Longitudinal Direction (z) = 13.00 Mpa
- Normal Stress in the Longitudinal Direction (x) = 15.20 Mpa
- Normal Stress in the Longitudinal Direction (y) = 81.80 Mpa

- Shear Stress in the Transverse & Vertical Direction (xy) = 6.85 Mpa
- Shear Stress in the Vertical & Longitudinal Direction (yz) = 13.30 Mpa
- Shear Stress in the Transverse & Longitudinal Direction (xz) = 2.10 Mpa

- Von-Mises Stress = 92.00 Mpa

Base Reactions in the Lift Core at the time of the maximum displacements:
- Longitudinal (z) Reaction at Base of Lift Core = 2,830 kN
- Transverse (x) Reaction at Base of Lift Core = 770 kN
- Vertical (y) Reaction at Base of Lift Core = 3,050 kN
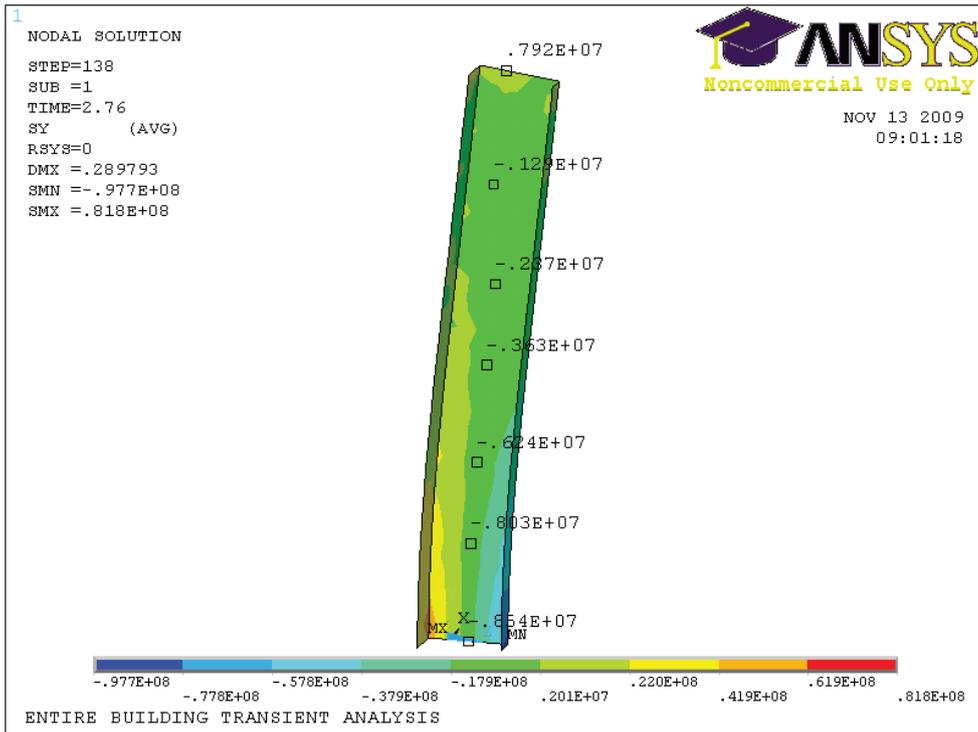
Figure 3.17– Contour Plot of Flexural Stress (y) in the Lift Core
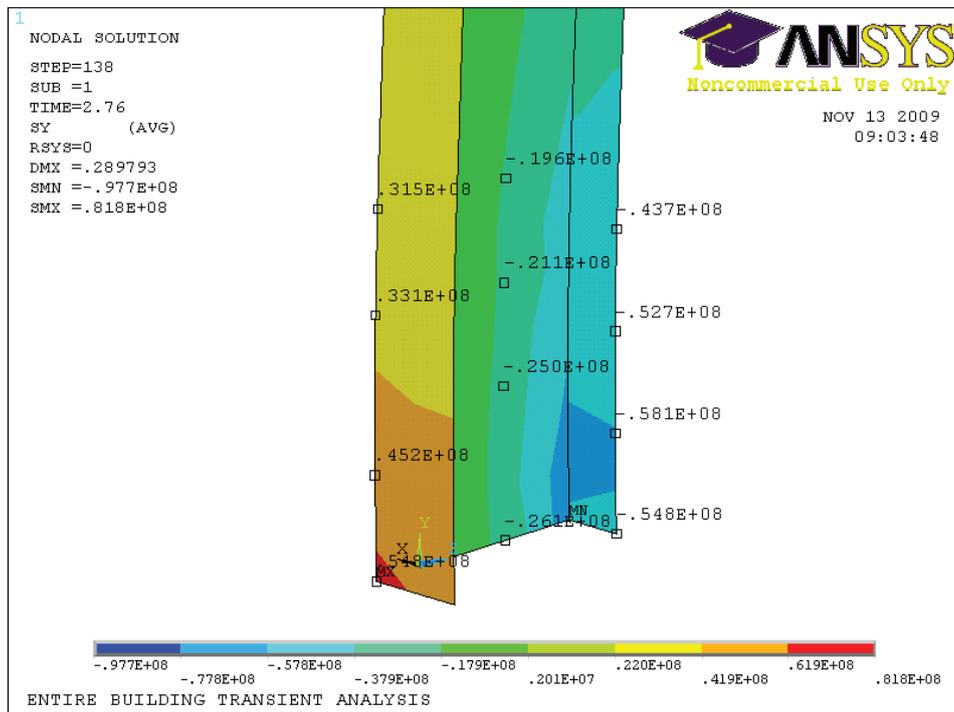
Figure 3.18 – Contour Plot of the Maximum Flexural Stress (y) in the Lift Core

3.8 Remodelled 7-storey Building

Figure 3.19 illustrates the plan view of the remodelled structure using four shear wall modules.

The intermediate analyses revealed that at least four modules (12 meters of walls in each direction of earthquake forces) are required to ensure the concrete strength is not exceeded under Kobe earthquake.

Table 3.5 summarises the results for inter-storey displacements. From the results we can see that the maximum inter-storey drift demand is 5.18 mm for Kobe and 3.47 mm for El-Centro earthquakes, respectively. The push over tests on Dincel wall units demonstrated that these limits can be met by the Dincel wall system.
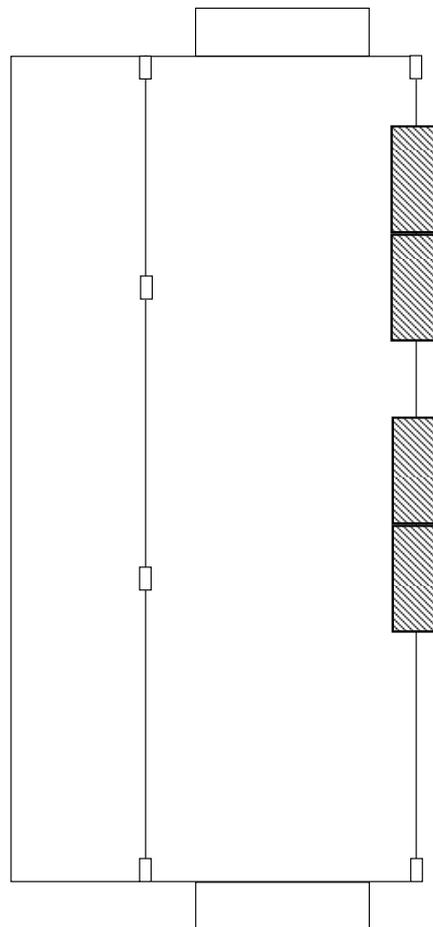
Figure 3.19 – Analysed half model with four modules

Table 3.5 - Maximum displacements of the remodelled building

El_centro Earthquake

Time	Displacement	Drift Displacement
4.54 (s)	(mm)	
L1	1.63	1.63
L2	4.29	2.65
L3	7.46	3.18
L4	10.91	3.45
L5	14.39	3.47
L6	17.71	3.32
L7	20.73	3.02

Kobe Earthquake

Time	Displacement	Drift Displacement
7.58 (s)	(mm)	
L1	2.70	2.70
L2	6.90	4.20
L3	11.81	4.91
L4	17.05	5.24
L5	22.23	5.18
L6	27.15	4.92
L7	31.60	4.46

Knowing the maximum inter-storey drift of 5.24 mm associated with the Kobe Earthquake, a series of FE analyses were also conducted on the u-shaped shear wall panel to determine the force required to produce the desired inter-storey drift and to also determine the natural frequency of the u-shaped panel to be compared later with the experimental values obtained from modal hammer tests.

3.9   FE Modelling of Push Over Test Panel

The purpose of this modelling was to compare the lateral stiffness of Dincel Wall system with a comparable conventional concrete wall. The results of this analysis are compared with the actual measured lateral stiffness of the push over Dincel Test Sample 'B'.

4   Experimental Testing of the U-shaped panels: Shake Table and Push over Tests

This part of the experimental program consisted of fabricating, curing and performing two sets of tests on two large wall specimens (2.8m high by 3.0 m wide) namely "A" and "B" using the Dincel system. The specimen "A" was centrally reinforced and specimen "B" reinforced with minor corner reinforcement only as shown on the drawings at Appendix A. The specimen "B" is referred to as unreinforced wall specimen hereinafter. The specimens were fabricated at the Structures Laboratory of the School of Civil and Environmental Engineering at UTS

DINCEL STRUCTURAL WALLING

with the assistance of Dincel staff. Two specially designed concrete bases were fabricated prior to erecting the walls on top of them. The form work and steel reinforcement for one such base is shown in Figure 4.1. Figures 4.2 and 4.3 show the polymer formwork and steel reinforcement prior to concrete pouring. After pouring of concrete the specimens were allowed to fully cure over an extended period of more than two months. After curing, the unreinforced wall specimen "B" was initially tested on the UTS shake table facility using the strong ground motion record of Kobe earthquake of 1995 (Figure 2.1) and El Centro, earthquake of 1940 (Figure 2.2) as input. The shake table tests were proved to be insufficient to determine the strength of the unreinforced wall specimen "B" in withstanding typical large magnitude earthquakes. This was due to very high stiffness of the specimens (fundamental frequency of about 48 Hz) resulting in rigid body motion of the specimen on the shake table with no relative displacement between the top and base of the specimen.   Figures 4.4 and 4.5 display unreinforced wall specimen "B" on UTS shake table ready to be tested. The specimens were fabricated with a solid concrete base as mentioned before and the base was in turn securely attached to the shake table prior to testing.
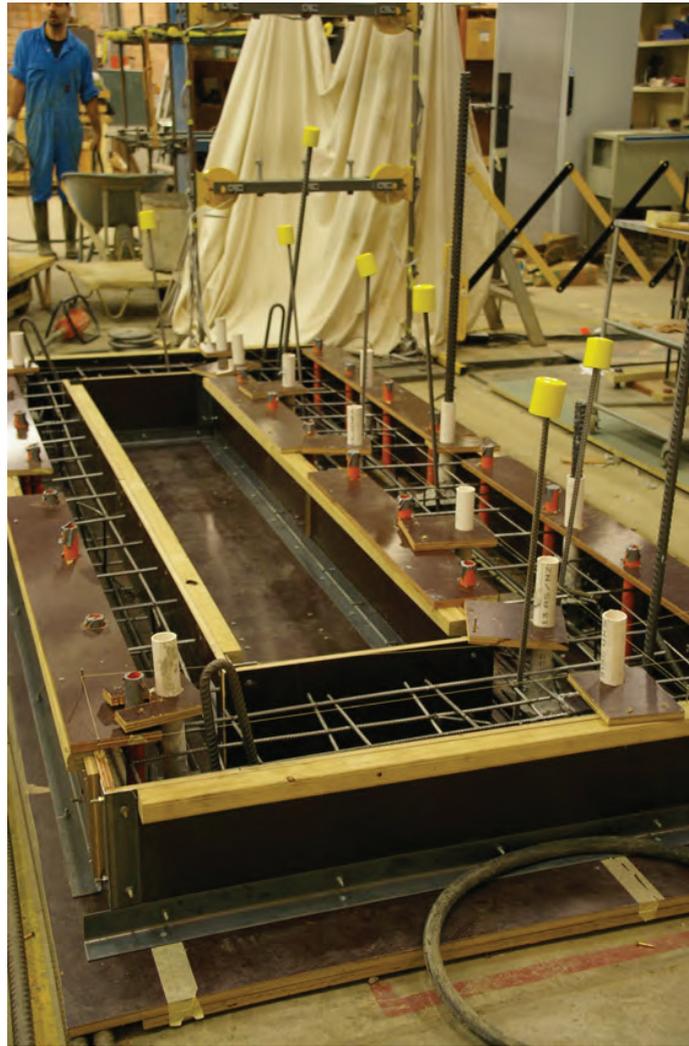
Fig 4.1 – Formwork and steel reinforcement for base structure
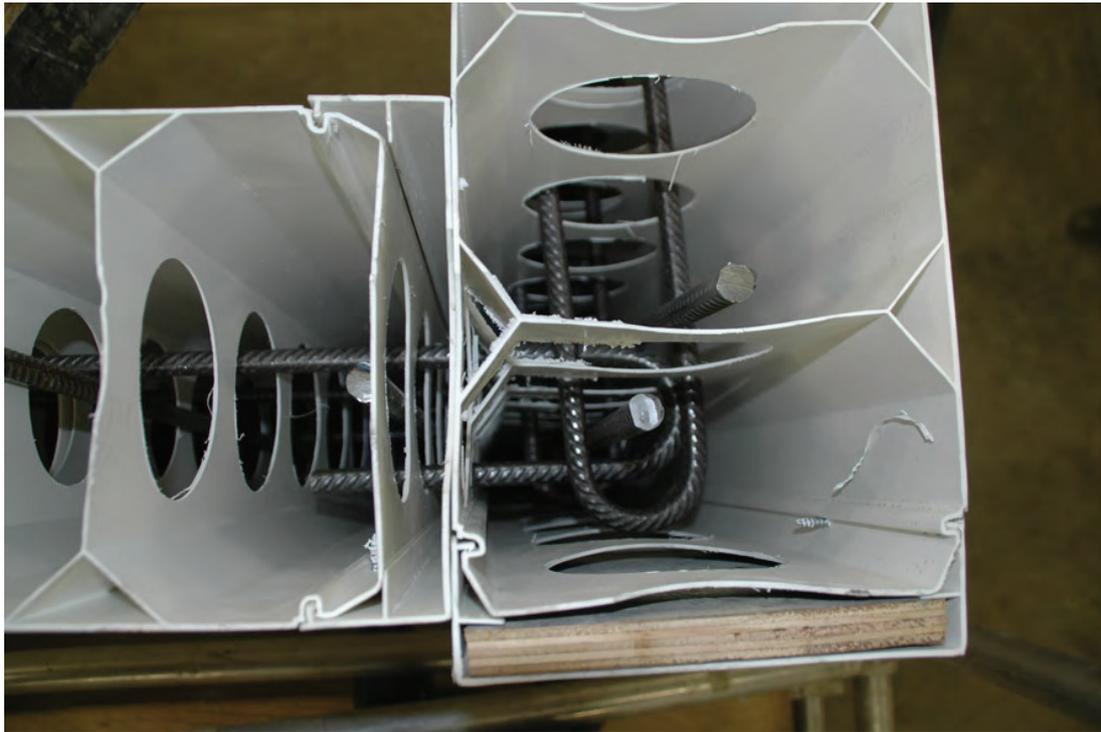
Fig 4.2 - Polymer forms and steel reinforcement – Wall corner

Fig 4.3 – Wall specimen ready for concrete pouring

Fig 4.4 – Unreinforced Wall unit and base on UTS shake table prior to testing

Fig 4.5 –Unreinforced Wall unit and base on UTS shake table prior to testing

Due to inability of the shake table tests to produce the desired storey drift, it was decided to subject these walls to push over tests to confirm their adequacy in providing the required displacement demand.

The two walls were then placed side by side on the strong floor of the structures laboratory at UTS and pushed sideways by two 100 tonne jacks, reacting against each other (Figure 4.6). The jacks provided "in-plane" loading conditions to simulate earthquake forces to be resisted by shear walls in buildings. Again, the base of both walls were securely attached to the strong floor using large steel beams and large high strength bolts to prevent sliding and lifting of the specimens during testing (Figures 4.7 and 4.8). Several displacement transducers were attached to the specimens and to the base to measure resulting displacements and to calculate the net in-plane inter-storey displacement of the walls from simple geometrical relations. The tests confirmed that the walls have adequate capacity to accommodate the displacement demand imposed by large earthquakes within the elastic range.

The lateral displacements for Sample 'B' of the push over test were then compared with FE modelling for a conventional plain concrete wall as previously described in Section 3.9. The comparison of the results conclude that Dincel Wall has similar lateral stiffness to a conventional plain concrete wall and that the polymer encapsulation of Dincel Wall does not reduce the lateral stiffness of the system.
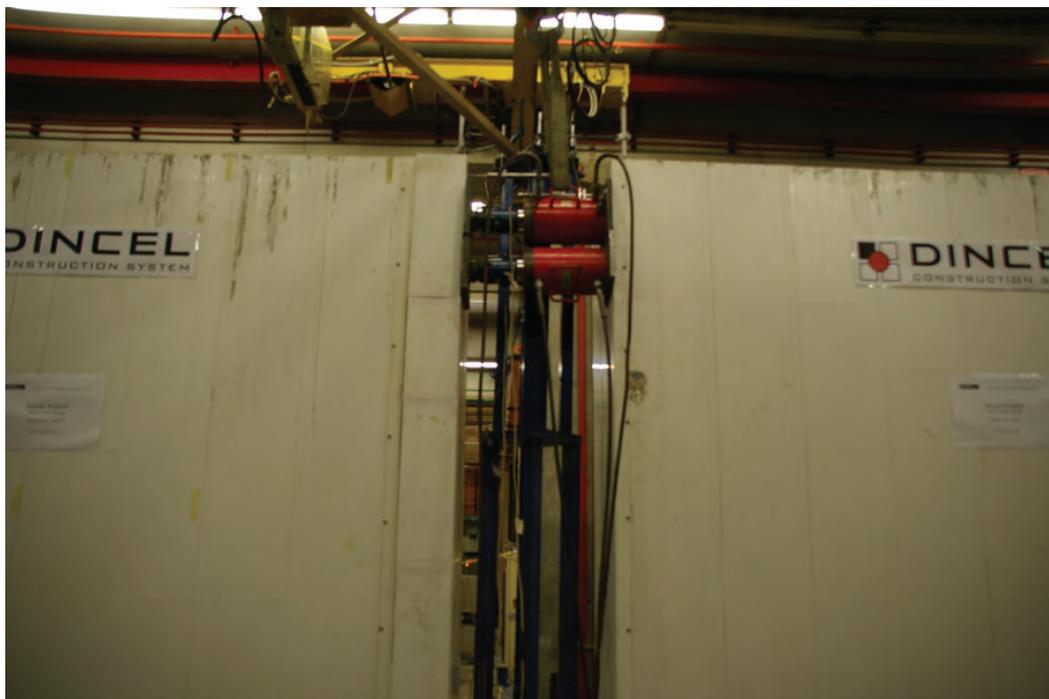
Figure 4.6 – Two Dincel walls on UTS strong floor ready for push over testing

Figure 4.7 – bases of two Dincel walls on UTS strong floor ready for push over testing

Figure 4.8 – Dincel Wall footing connection to strong floor

4.1 Hammer Test

To verify the adequacy and accuracy of the FE model of the U-shaped specimen, an experimental investigation was carried out on the specimen to determine its actual natural frequencies and compare them with those obtained from FE analysis A Modal Hammer Test was carried out on the lift core segment to determine the structures natural frequencies and mode shapes.

A simple description of the procedure is that it uses a specially calibrated modal sledge hammer to excite the structure, which subsequently allows the natural frequencies and mode shapes to be extracted from the structure's 'free' vibrations following the impact. Accelerometers which are strategically positioned on the structure are used to measure the vibrations over a short period of time, and subsequently send the results to a data acquisition system. The data acquisition system then converts the readings from accelerations in the time domain to Frequency Response Functions (FRF) in the frequency domain following a Fast Fourier Transformation (FFT). From the FRFs, the natural frequencies are extracted from the peaks on the graph. Finally, modal analysis software is used to extract the structure's mode shapes from the natural frequencies.

The process of the Hammer Testing was repeated several times and the structure was struck at different locations. The objective of this was to excite all possible modes of vibrations.

Five such modes were determined from hammer tests and were compared with those obtained from the FE analysis. The results are given in Table 4.1. From this table it is clear that the correlation between the experimental and FE analyses is very good for the first two modes, particularly the first mode.

Table 4. 1 – Results of Natural Frequency Calculations

Mode	Finite Element (Hz)	Experimental (Hz)	|Difference| (Hz)	Error
1	48.27	49.09	0.82	1.67%
2	69.07	72.59	3.52	4.85%
3	83.69	96.58	12.89	13.35%
4	98.82	136.86	38.04	27.79%
5	148.71	127.85	20.86	16.32%

The 12 lb modal hammer used for these tests is shown in Figure 4.9.   Figure 4.10 shows the hammer test in progress.
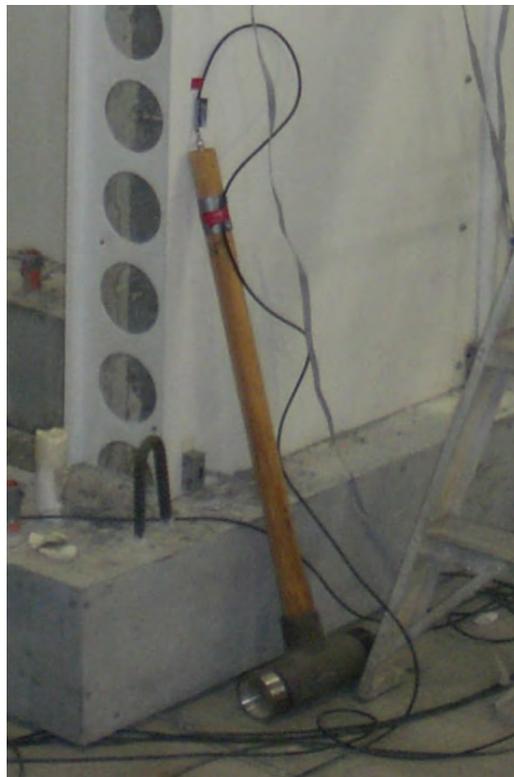
Fig 4.9 - The 12 lb Modal Hammer used for hammer tests

Fig 4.10 – Conducting Hammer Test on the specimen

5 Analysis and Testing of High Narrow Specimens Subjected to Out-of-Plane Loading

The analytical and experimental studies of the U-shaped specimens loaded in plane and acting as a shear wall, although useful, did not reveal the advantages and potential superiority of Dincel system over conventional concrete walls to extreme seismic loading when failure and collapse is likely due to very large inter-storey displacements. The U-panel push over tests showed that the Dincel system can accommodate the required 5.3 mm storey drift under in-plane loading conditions. But this does not mean a conventional concrete wall with adequate steel reinforcement cannot accommodate the same displacement demand.

To address this shortcoming, and in consultation with Dincel engineers, it was decided to fabricate, analyse and test two flexible specimens and subject them to severe shaking near resonance conditions. The specimens were of identical sizes, 4 m high, 640 mm wide and 195 mm thick. One specimen was fabricated using the Dincel system and the other one using reinforced concrete as a conventional system. Both systems were reinforced at the centre of the wall for exact comparisons. The main objective of this exercise was to establish and directly compare the resilience of

the Dincel wall with that of the conventional wall in sustaining large deformations, well in excess of what the codes allow. To achieve large deformations, it was therefore necessary to expose the specimens to out of plain loads on the UTS shake table at or near resonance conditions.

The international standards have set out the following criteria for inter-storey drifts and possible consequences of such drifts. This is given in Table 5.1 below.

Fully Operational	Maximum inter-storey drifts < 0.2%
Operational	Maximum inter-storey drifts < 0.5%
Life Safe	Maximum inter-storey drifts < 1.5%
Near Collapse	Maximum inter-storey drifts < 2.5%
Collapse	Maximum inter-storey drifts > 2.5%

Table 5.1 - Performance Levels (FEMA 273/274, 1997)

Therefore, the main objective of these tests was to subject the two specimens to the maximum possible displacements and observe their behaviour.

5.1 Theoretical Evaluation of Dynamic Response of Conventional Concrete Wall to Dynamic Excitation

The idea behind both Dincel and conventional walls was to test them on shaker table with a frequency close to resonance frequency leading to maximum displacements, maximum inertia forces and hence maximum base shear forces. To design a suitable supporting structure, the maximum base shear force acting on supporting structure has to be determined and hence calculated from principles of mechanics and presented in at Appendix B. Frequency and displacement of the table are also evaluated as part of these calculations . Dynamic characteristics such as first natural frequency and damping ratio were also evaluated based on theoretical approach using design characteristics of the walls. Actual values were then obtained using "hammer test" and compared to the theoretical ones in the results comparison table.

According to calculations presented at Appendix B, the walls have a first uncracked first natural frequency of about 10 Hz.

5.2   Design of the Supporting Structure

The supporting structure is designed to resist force and bending moment acting from the wall during excitation. It is designed in a way that it eliminates any slip between their parts, and between supports and the shake table. Any additional gap between the wall and supporting elements may create higher damping of the wall during excitation as well as excessive local stress in concrete adjacent to the supports. Forces acting on each element were calculated using finite element analysis. Results of the analysis are presented at Appendix C.

Based on the FE analysis and using the provisions of the Australian Steel Code, a conservative supporting structure made of steel was designed and fabricated at the UTS Faculty of Engineering and Information Technology Workshop. Figures 5.1 - 5.3 illustrate the shake table testing set up for the walls.
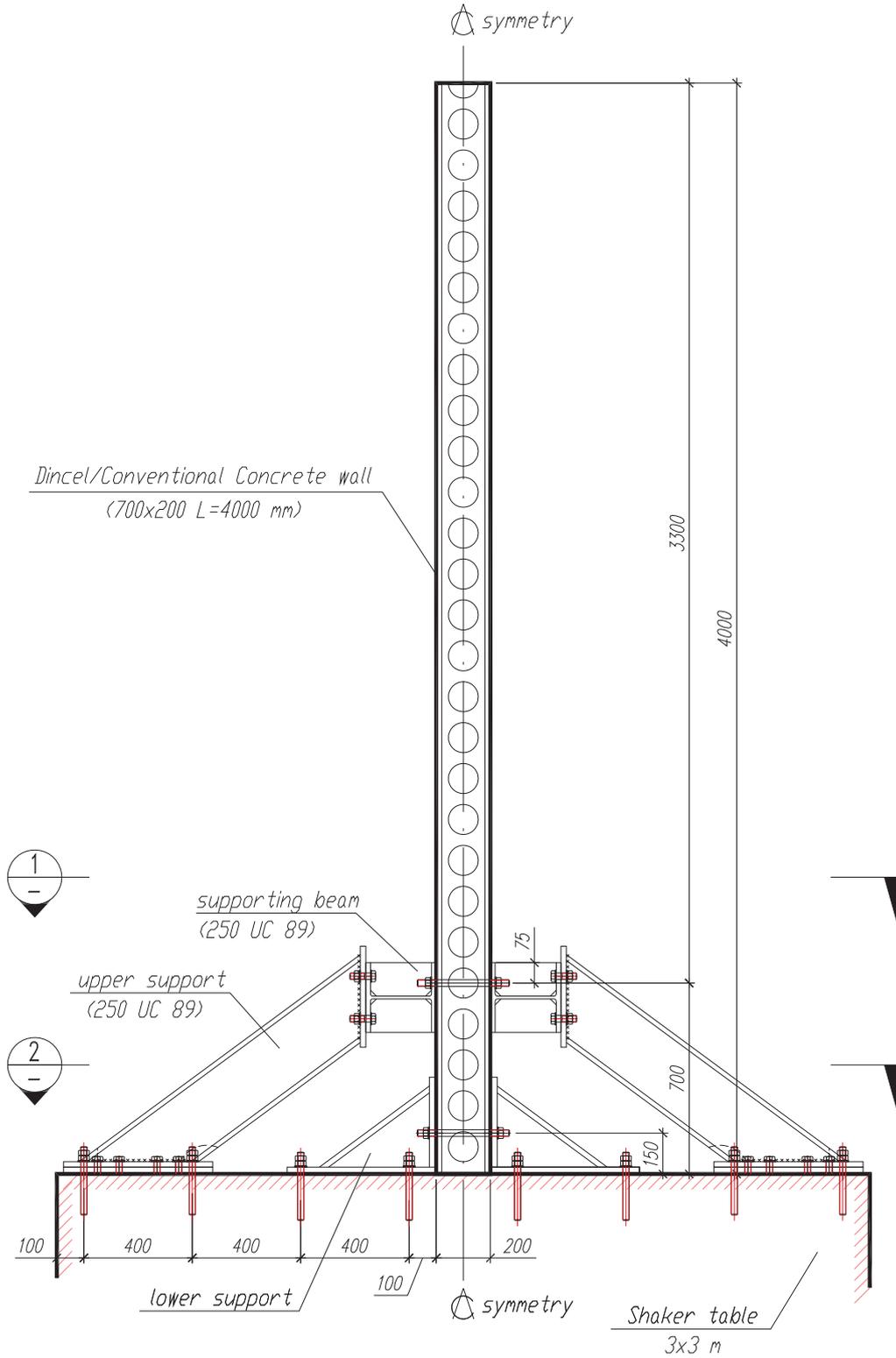
Dincel wall Dynamic Testing Setup. Side view.

Fig 5.1- Dincel Wall Shake Table Testing Set up, side view
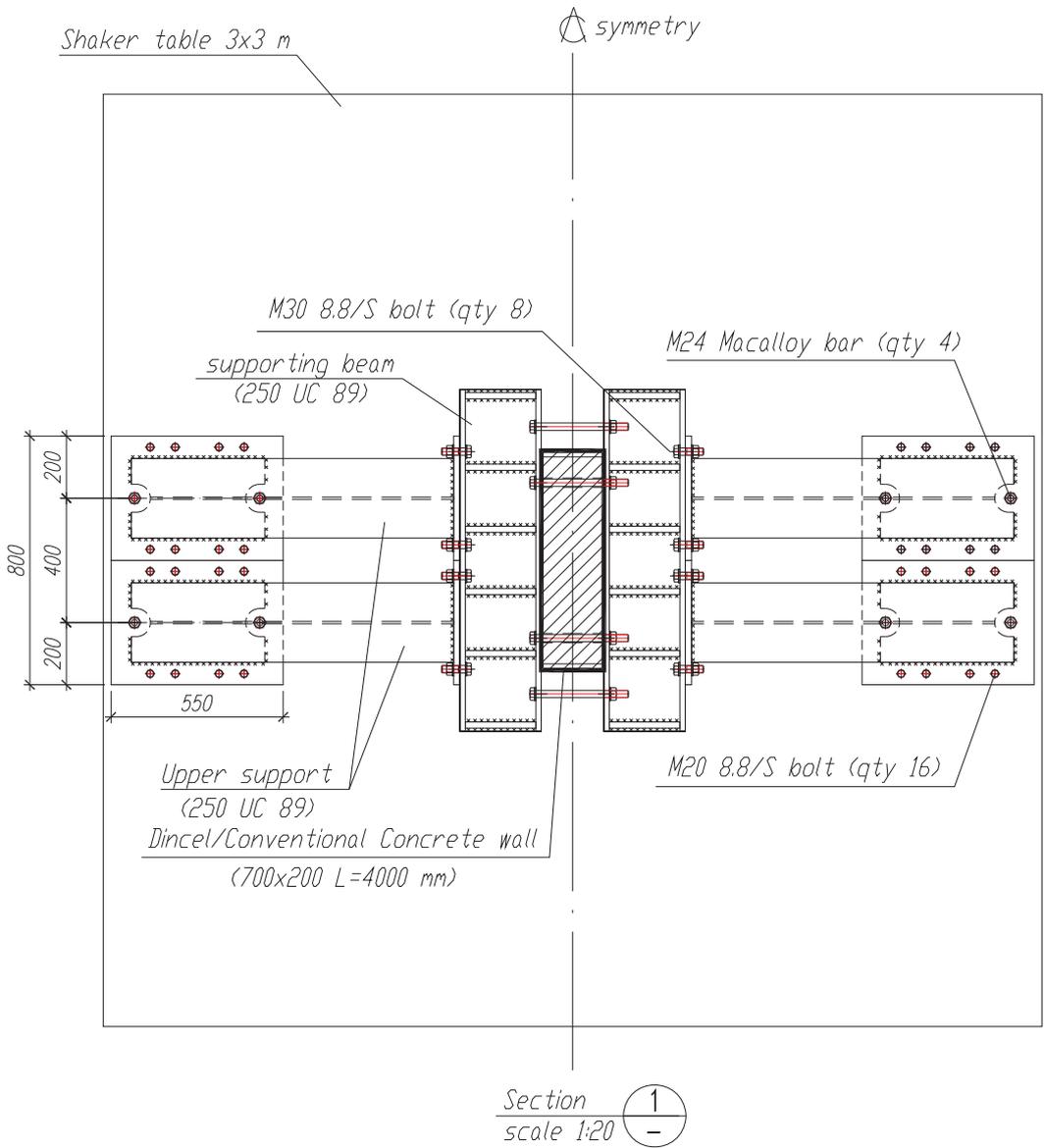
Fig 5.2- Dincel Wall Shake Table Testing Set up, section 1

symmetry

lower support

M24 Macalloy bar (qty 4)

800
400
800

550

550

Dincel/Conventional Concrete wall
(700x200 L=4000 mm)
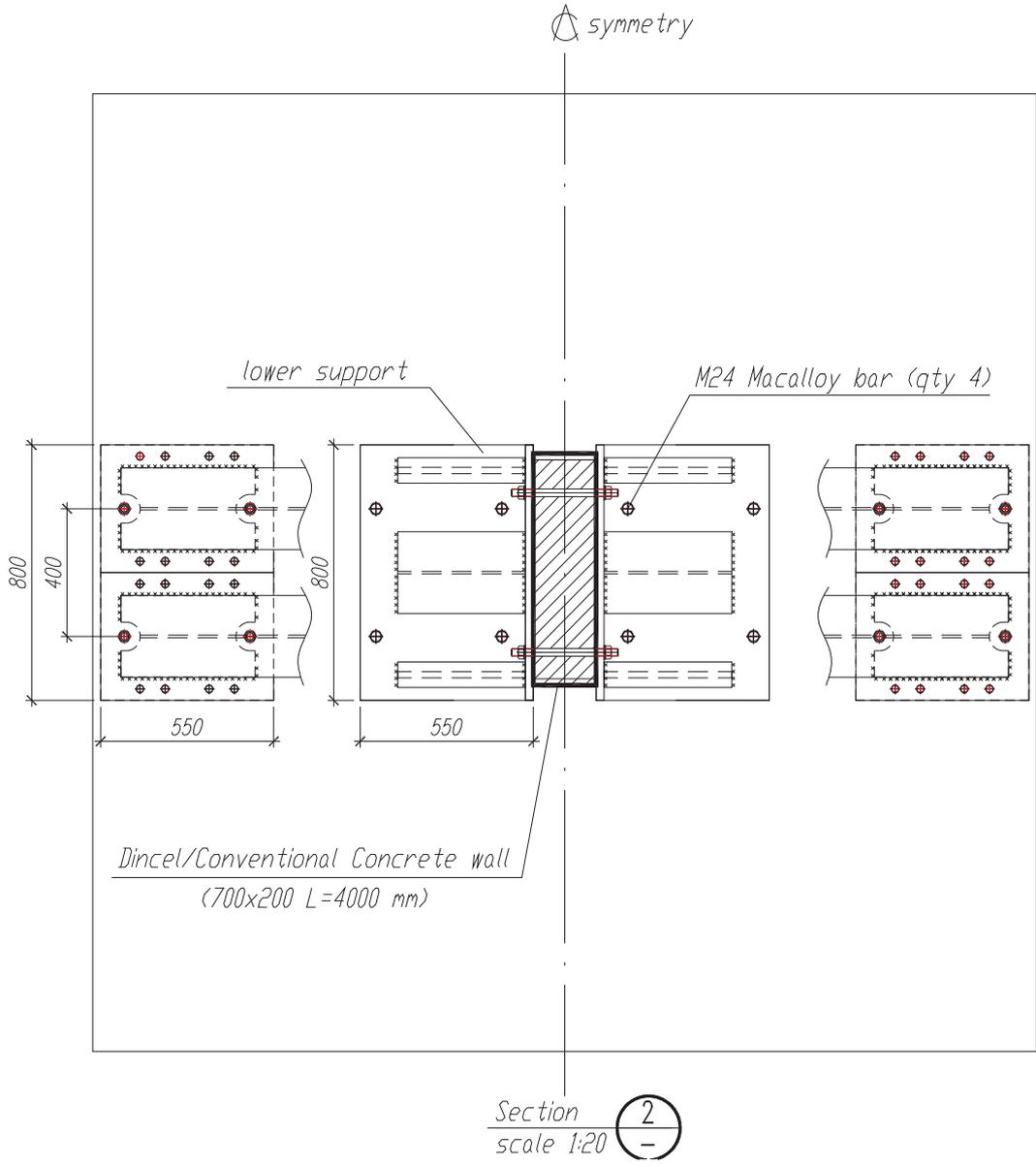
Section
scale 1:20   2 —

Fig 5.3- Dincel Wall Shake Table Testing Set up, section 2

5.3 Testing of the Two Walls

The walls were tested one after the other. Dincel wall was tested first followed by testing of the conventional wall. Figures 5.4 and 5.5 show the conventional wall secured on the shake table and ready to be tested. The set up for Dincel wall was identical to Figure 5.4 and 5.5.

Fig 5.4- Conventional system Sample 'D' set up on UTS Shake Table

Fig 5.5 - Test set up on UTS Shake Table

Figures 5.6 and 5.7 show some details of the support structure and the instrumentation used.

Fig 5.6 - Test set up (close up of the supporting structure)
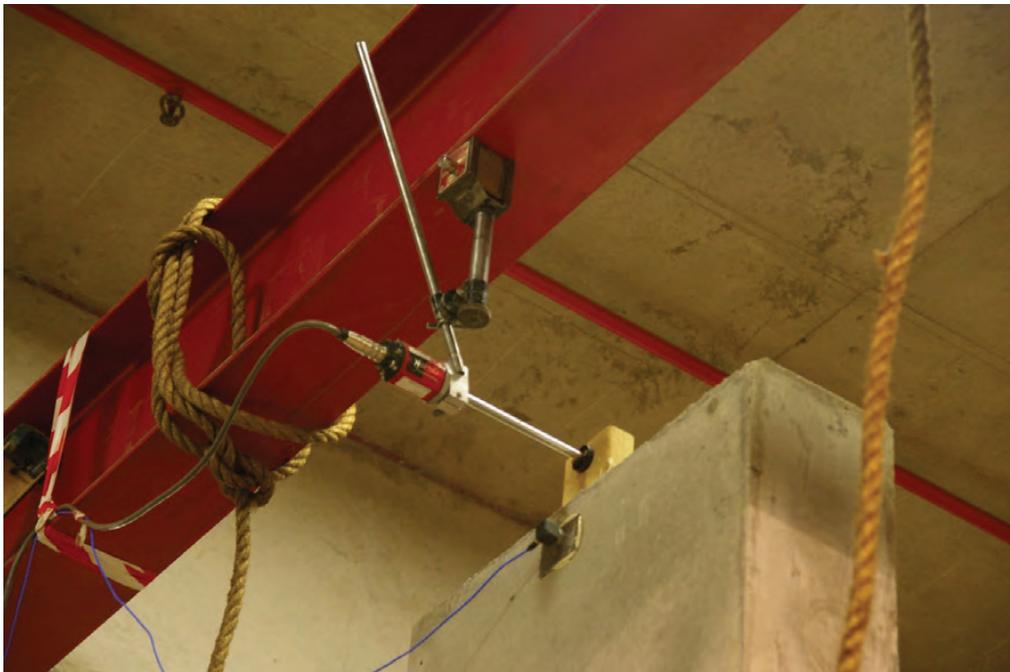
Fig 5.7 - Test set up (Dynamic LVDT and Acceleometer attached to the top of the wall)

Fig 5.8 – Dincel System Sample 'C' set up on UTS Shake Table

5.4 Test Results

5.4.1 Dynamic Properties of the Walls - Dincel Wall

Natural frequency results for Dincel Wall tests were obtained at 3 stages of the test using hammer tests:

- An uncracked state (before excitation);
- Minor cracked state (cross section of the wall cracked at the distance x=0.7 m from the base;
- Cracked state (after the test being executed, cracking of the cross section of the wall at distances x=0.7 m above the shake table, x=1.15 m above the shake table. (see Figure 5.14)

Observations:

Due to extensive crack formation, first natural frequency changed from 9.2Hz prior to shake table testing (Fig. 5.8), to 7.44Hz (Fig. 5.9) after minor shaking resulting in minor cracking and to 3.6Hz (Fig. 5.10) at the end of the test after the formation of major cracks. It should be noted that after first cracks were formed the wall had no longer a uniform stiffness throughout its length. Continuous cracks throughout the section created "semi hinges" which influenced dynamic performance and properties of the structure such as change of the natural frequency (first, second, etc.), flexibility at the places of crack formation, and increased damping. Variation of dynamic properties was creating different dynamic response such as mode of vibration and maximum displacement at the top of the wall.

Cracking also increased the damping of the system. The corresponding damping ratios were calculated from the free vibration displacement time histories following each hammer test using the logarithmic decrement approach. The damping ratio for the uncracked state was calculated as 0.67% of critical damping (see Fig 5.11), for the minor cracked state it was calculated as 1.21% (see Fig 5.12) and for the major cracked state (at the conclusion of the test) was calculated as 2.48% (see Fig. 5.13).

DINCEL
STRUCTURAL WALLING

Dincel Wall Hammer Test.
Frequency Response Function. Uncracked state.
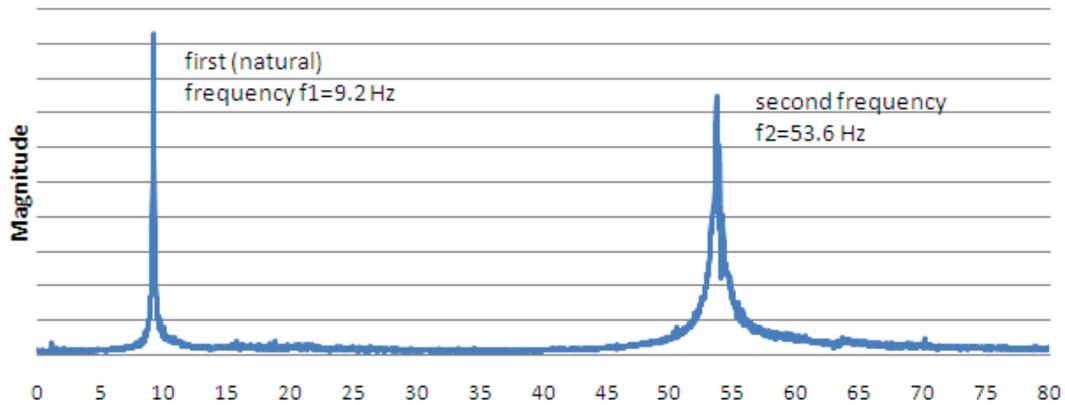
Fig 5.8 – Frequency Response Function showing a fundamental frequency of 9.2 Hz in uncracked state (*uncracked state – Dincel wall*)

Dincel Wall Hammer Test.
Frequency Response Function. Minor Cracked State.
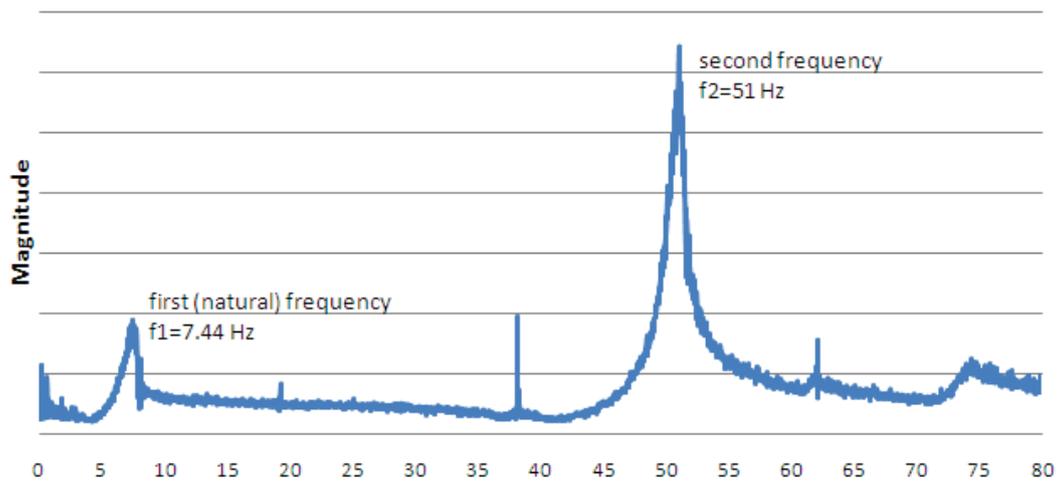
Fig 5.9 – Frequency Response Function showing a fundamental frequency of 7.44 Hz in minor cracked state (*minor cracked state – Dincel wall*)

Dincel Wall Hammer Test.
Frequency Responce Function. Major Cracked State.
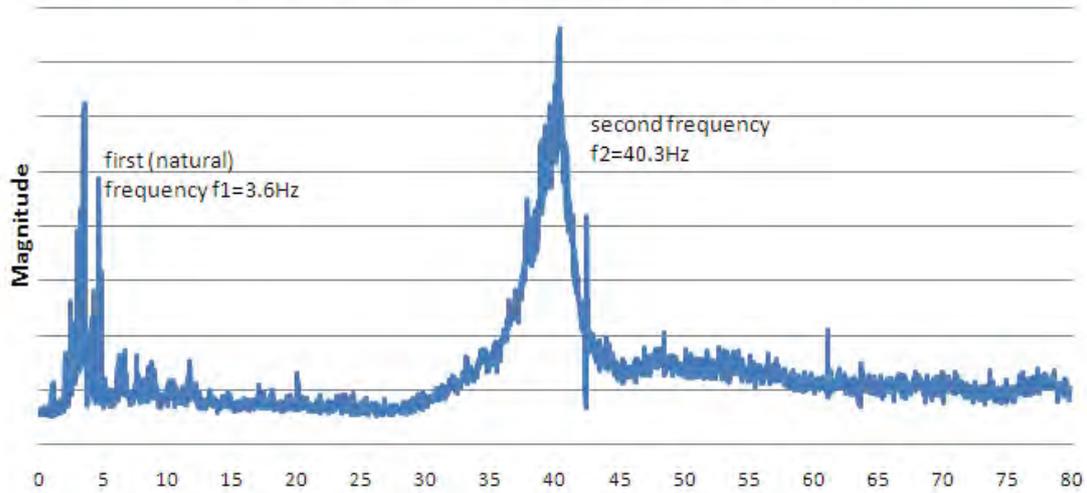
Fig 5.10 – Frequency Response Function showing a fundamental frequency of 3.6 Hz in major cracked state (*major cracked state – Dincel wall*)

Dincel Wall. Uncracked State. Free Vibration.
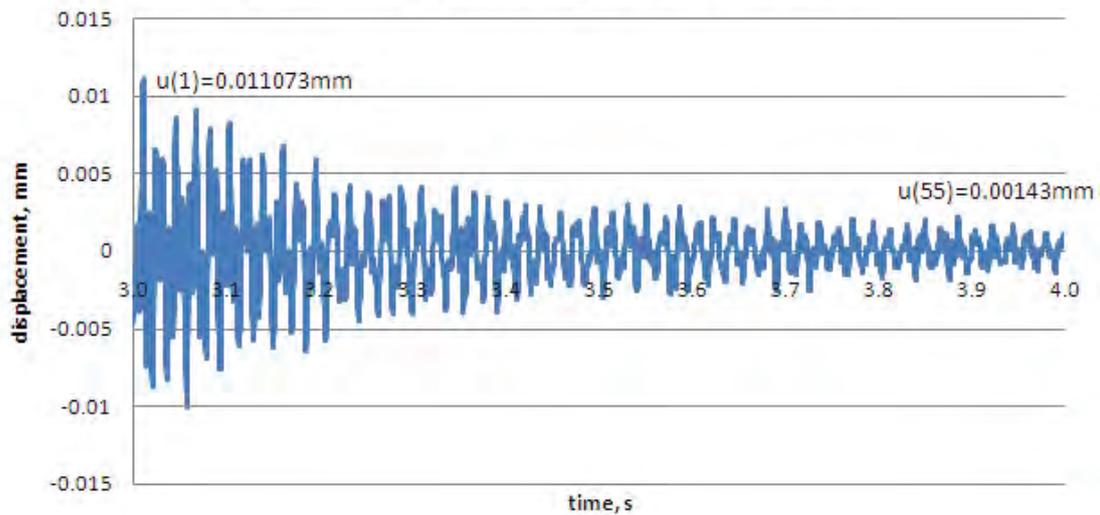
$$\xi = \frac{\ln(0.01143/0.0011143)}{2\pi \cdot 55} = 0.0067$$

Fig 5.11 – Free vibration displacement time history following hammer test prior to testing (*uncracked state – Dincel wall*)

Dincel Wall. Minor Cracked state. Free vibration.
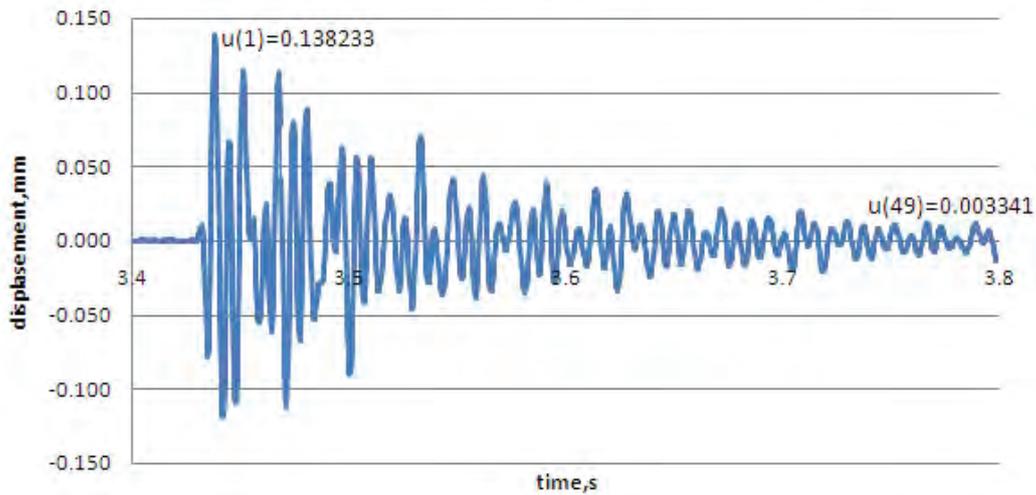
$$\xi = \frac{\ln(0.138233/0.003341)}{2\pi \cdot 49} = 0.0121$$

Fig 5.12 – Free vibration displacement time history following hammer test prior to testing
(*minor cracked state – Dincel wall*)

Dincel Wall. Major Cracked state. Free vibration.
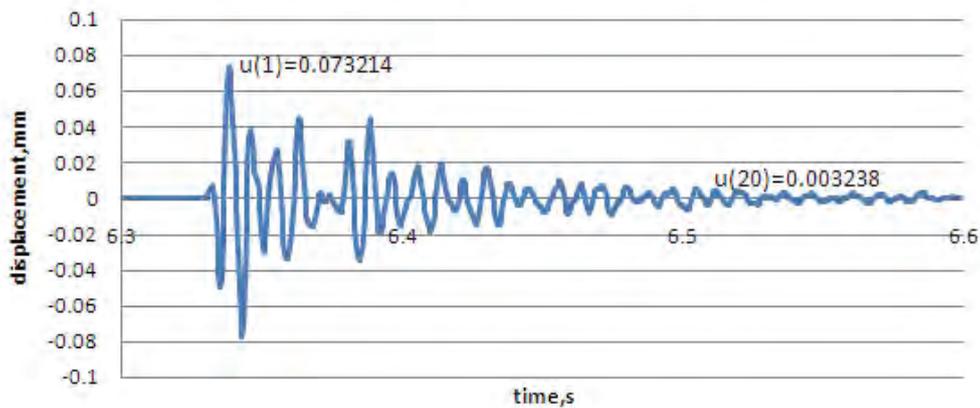
$$\xi = \frac{\ln(0.073214/0.003238)}{2\pi \cdot 20} = 0.0248$$

Fig 5.13 – Free vibration displacement time history following hammer test prior to testing
(*major cracked state – Dincel wall*)

DINCEL
STRUCTURAL WALLING

Following the conclusion of the tests Figure 5.14 below shows the cracks and the details of those cracks at the exposed concrete face of the test panel.

Figure 5.14 (a) Dincel Sample 'C' after testing

Figure 5.14 (b) Dincel Sample Crack at X = 700mm

Figure 5.14 (c) Close Up View of Crack at X = 700mm
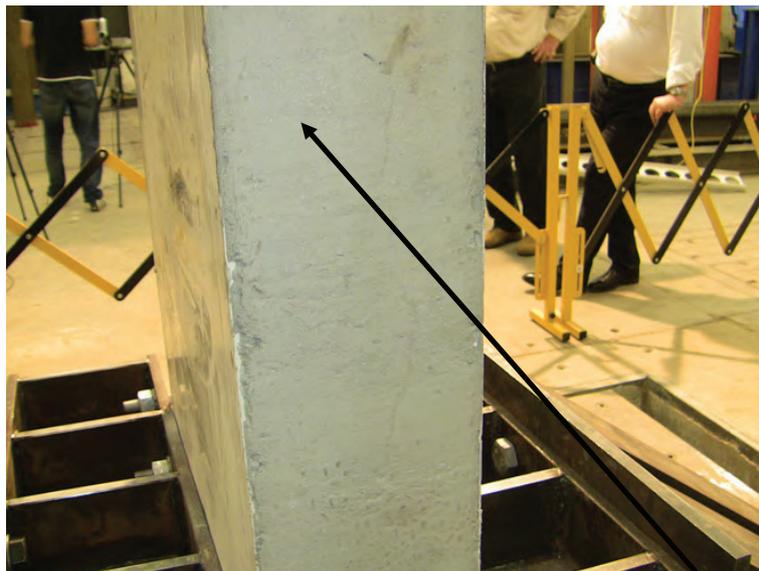
Figure 5.14 (d) Dincel Sample Crack at X = 1150mm

Figure 5.14 (e) Close Up View of Crack at X = 1150mm

Fig 5.14 – (a), (b), (c), (d) and (e)

Visible cracks in Dincel wall following the shake table tests (details)

5.4.2 Dynamic Properties of the Walls – Conventional Wall

The results of the shake table tests pertaining to the conventional wall are presented in this section. Similar observations to those for the Dincel wall can be observed.

As before, the natural frequency results for the conventional wall tests were obtained at 3 stages of the test using hammer tests:

- An uncracked state (before excitation);

- Uncracked to minor cracked state (small hairline cracks are observed at different locations along the wall);

- Major cracked state (after the test being executed, extensive cracking of the cross section of the wall at distances x=0.7 m, x=1.15 m minor cracking at x=0.15 m, x=1.48 m) (see Figures 5.21 and 5.22).

Observations:

Due to extensive crack formation, the first natural frequency changed from 10.2 Hz prior to shake table testing (Fig. 5.15), to 9.80 Hz at the "uncracked- minor cracked" state (Fig. 5.16) to 2.37 Hz (Fig. 5.17) at the end of the test after the formation of major cracks. As before, after first cracks were formed the wall no longer had a uniform stiffness throughout its length. Continuous cracks throughout the section created "semi hinges" which influenced the dynamic performance and properties of the structure such as change of the natural frequency (first, second, etc.), flexibility at the places of crack formation, and increased damping. Variation of dynamic properties was creating different dynamic response such as mode of vibration and maximum displacement at the top of the wall, as mentioned for the Dincel wall.

Cracking also increased the damping of the system as expected. The corresponding damping ratios were calculated from the free vibration displacement time histories following each hammer test using the logarithmic decrement approach.   The damping ratio for the uncracked state was calculated as 1.18% of critical damping (see Fig 5.18), for the minor cracked state it was calculated as 1.21% (see Fig 5.19) and for the major cracked state (at the conclusion of the test) was calculated as 1.7% (see Fig. 5.20).

Conventional Wall Hammer Test. Frequency Response Function. Uncracked State.

first (natural) frequency f1=10.2 Hz

second frequency f2=59.2 Hz
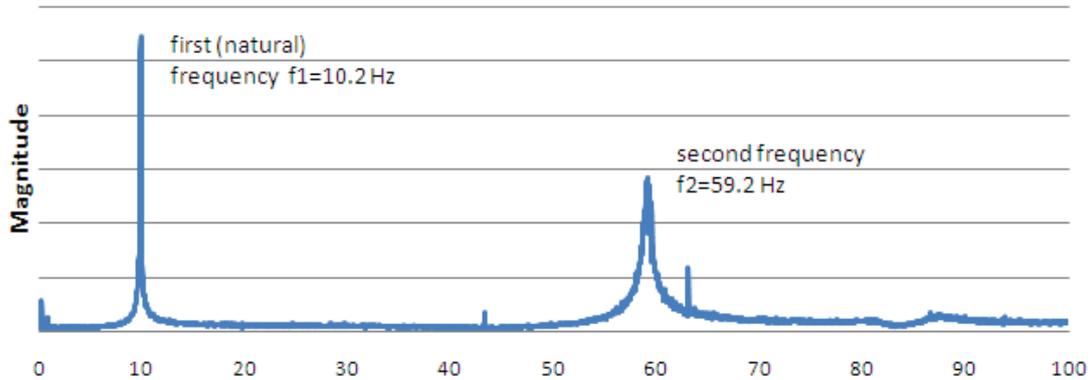
Fig 5.15 – Frequency Response Function showing a fundamental frequency of 10.2 Hz in (*uncracked state – Conventional wall*)

Conventional Wall Hammer Test. Frequency Response Function. Uncracked - Minor Cracked State.

first (natural) frequency f1=9.8 Hz

second frequency f2=57.8 Hz
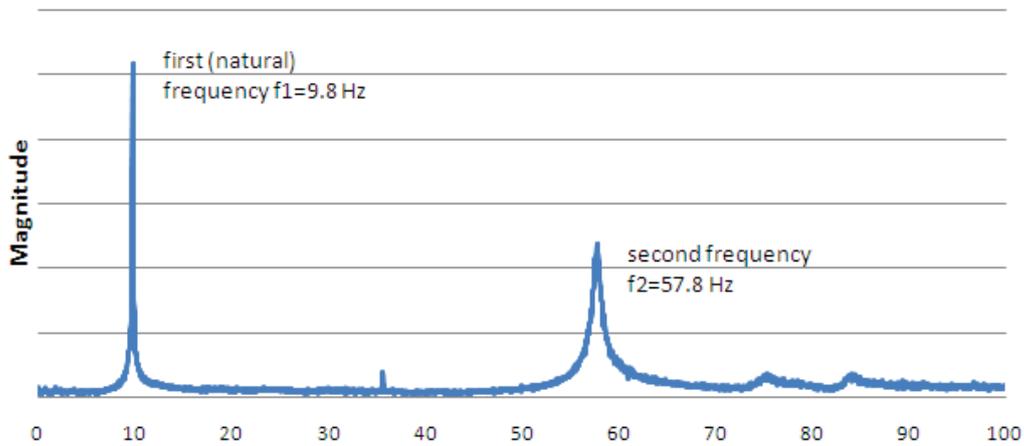
Fig 5.16 – Frequency Response Function showing a fundamental frequency of 9.8 Hz in (*uncracked-minor cracked state – Conventional wall*)

Conventional Wall Hammer Test. Frequency Response Function. Major Cracked State.
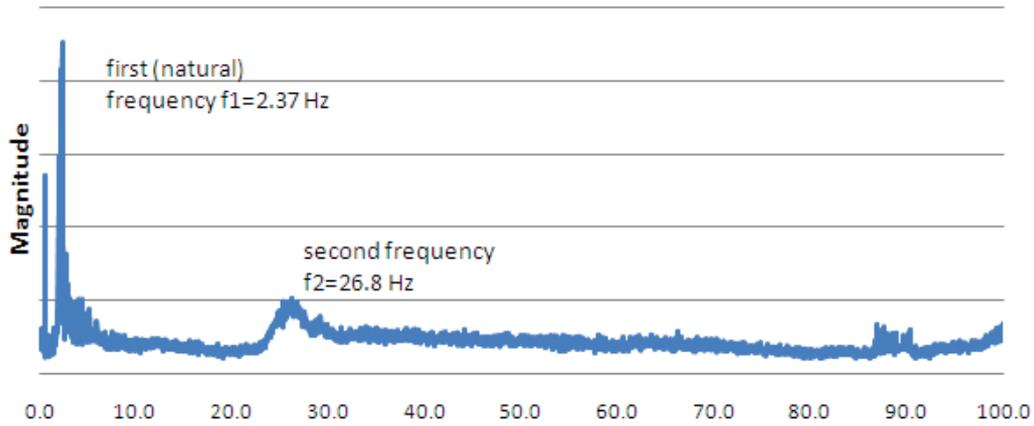
Fig 5.17 – Frequency Response Function showing a fundamental frequency of 2.37 Hz in
(*major cracked state – Conventional wall*)

Conventional Wall. Uncracked State. Free vibration.
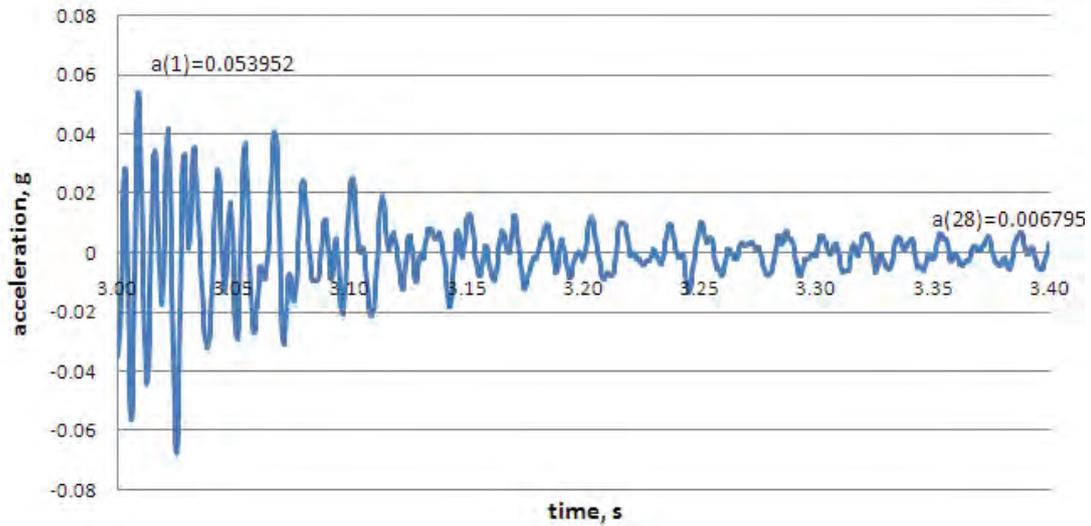
Fig 5.18 – Free vibration displacement time history following hammer test prior to testing
(*uncracked state – Conventional wall*)

Conventional Wall. Uncracked - Minor Cracked State. Free Vibration.
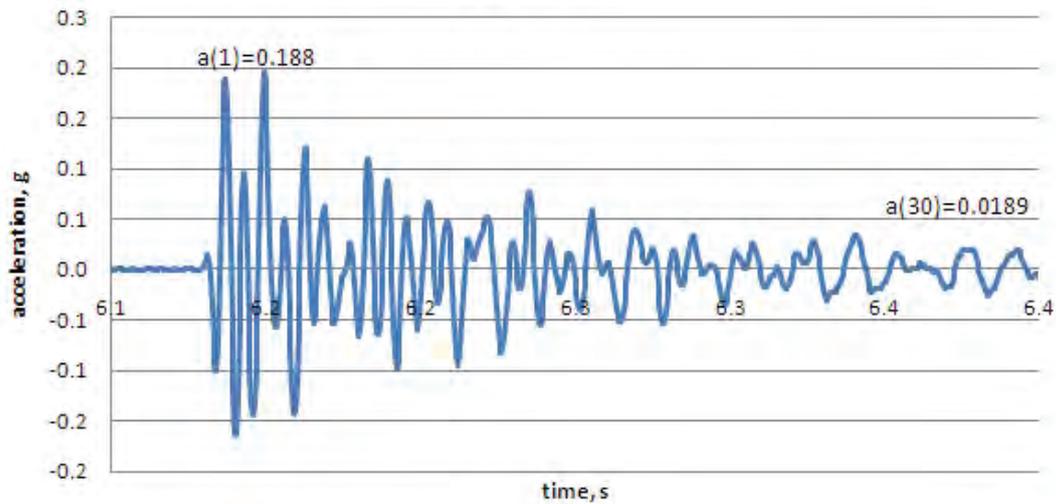
Fig 5.19 – Free vibration displacement time history following hammer test prior to testing
(*uncracked-minor cracked state – Conventional wall*)

Conventional Wall. Major Cracked State. Free vibration.
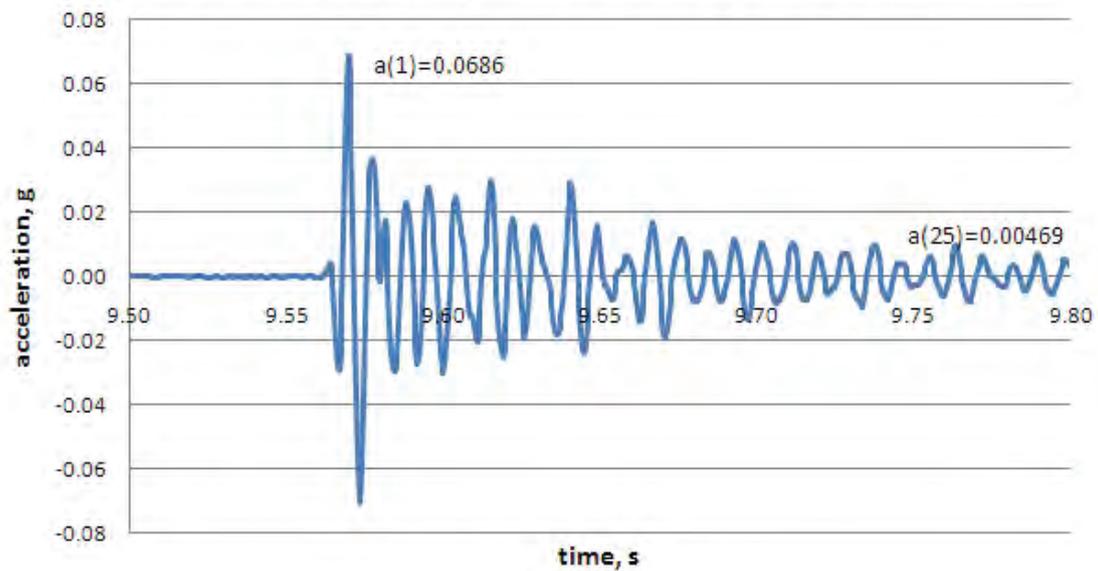
Fig 5.20 – Free vibration displacement time history following hammer test prior to testing
(*major cracked state – Conventional wall*)

It is worth mentioning that the conventional wall initially had higher first natural frequency than it was observed for the Dincel wall due to higher stiffness but it reduced its first natural frequency at the end of the test more than the Dincel wall with the same amount of damage. This is due to confinement of concrete by polymer encapsulation for the Dincel wall which has a stiffening effect after concrete is damaged.

Figures 5.21 and 5.22 show the conventional wall at the conclusion of the tests with several cracks appearing.

DINCEL
STRUCTURAL WALLING

Fig 5.21 - Conventional wall at the conclusion of the tests
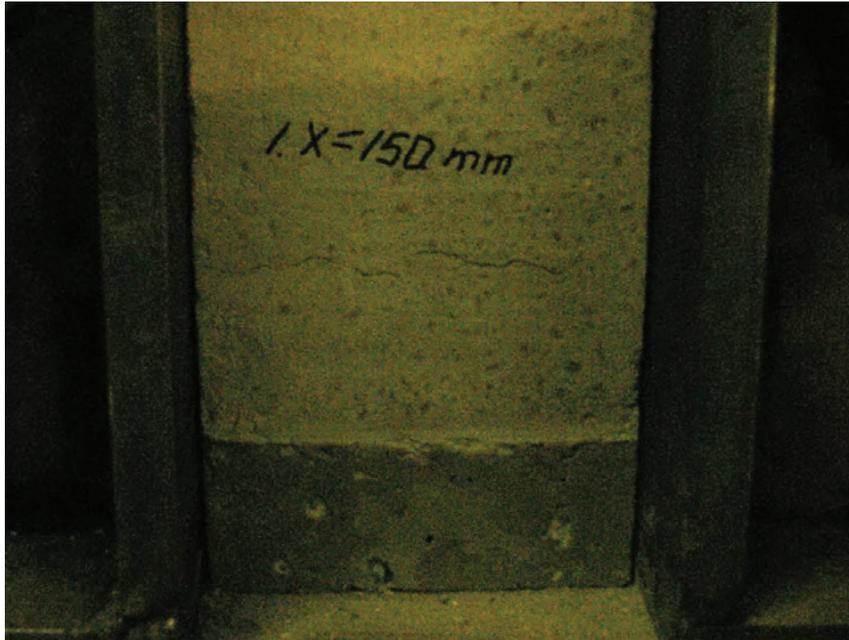
(a)
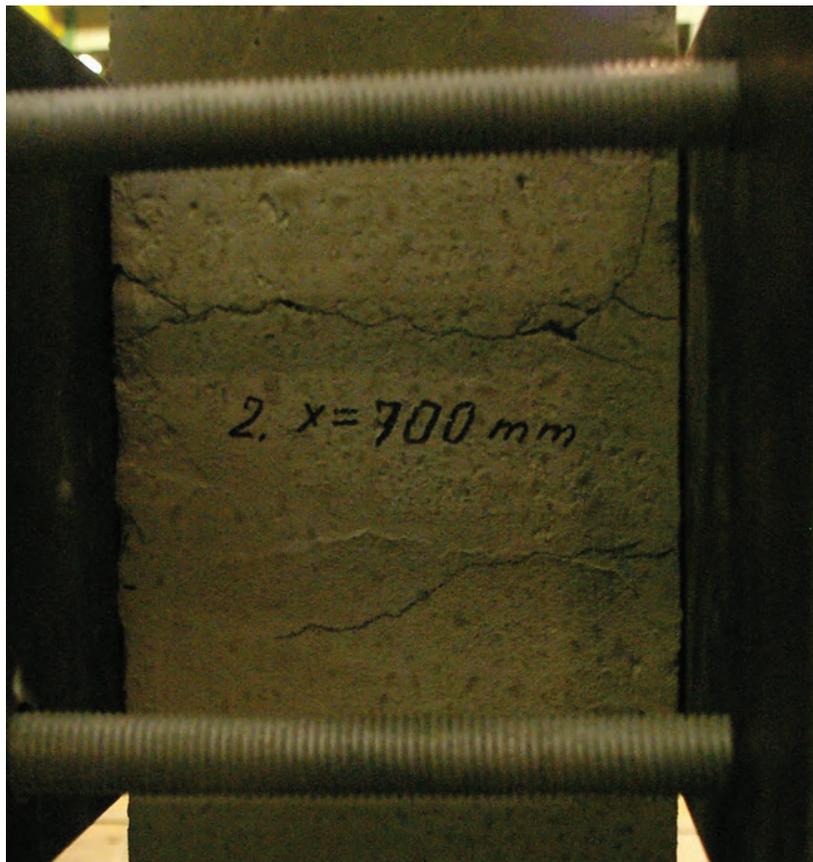
(b)

(c)

(d)

Fig 5.22 - Conventional wall at the conclusion of the tests (details)

5.4.3 Response of the Structure to Dynamic Excitation - Dincel Wall

The first natural frequency of the wall in the uncracked state was 9.2 Hz which dropped down to 3.6 Hz after the test was completed. The idea of each excitation was to "chase" the first natural frequency and come closer to resonance fequency but still comply with safety requirements of the test. Deflection at the top of the wall during the second excitation reached 9.6 mm before wall cracked (it was expected to have 6.6 mm according to hand calculations with an assumption of "unconfined" plain concrete work. After the first cracking was reached the wall changed its deformed shape of vibration (see Fig. 5.23).

Deformed Shape of Vibration.

Before Cracking   **After Cracking**

top displ.   top displ.

3300   3300

4000   4000
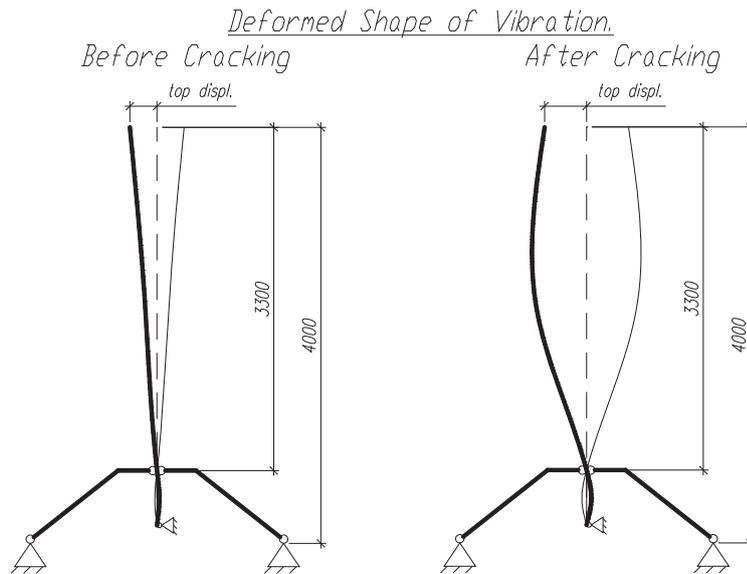
Fig 5.23 – Deformed vibration mode before and after cracking

Figure 5.24 conveys vital information in terms of maximum top displacement relative to shake table displacement. We can see that as the first natural frequency drops due to increased severity of cracking, the relative displacement increases to a maximum value of 145 mm before the specimen was declared fully damaged and the test stopped. This displacement value represented storey drift of 4.4% (145/3,300) which is well in excess of 2.5% as the failure drift based on Table 5.1 figures. Even at this displacement value the Dincel wall was deemed as safe in terms of possible threat to human life, clearly demonstrating the advantage of using Dincel wall for additional safety and where large displacements demands are required for safe aseismic design.

In Fig 5.24, five stages of excitation and the corresponding responses are shown. For each stage, the corresponding frequency, damping ratio and maximum relative displacement are shown. The maximum relative displacement at the top of the wall is shown in fig. 5.25.

DINCEL
STRUCTURAL WALLING

Displacement time histories of the top of the wall measured by a dynamic LVDT and those for the shake table are shown in Figures 5.26 to 5.30 for excitation levels 1 to 5, respectively.

Fig 5.24 – Frequency versus maximum displacement for five excitation states
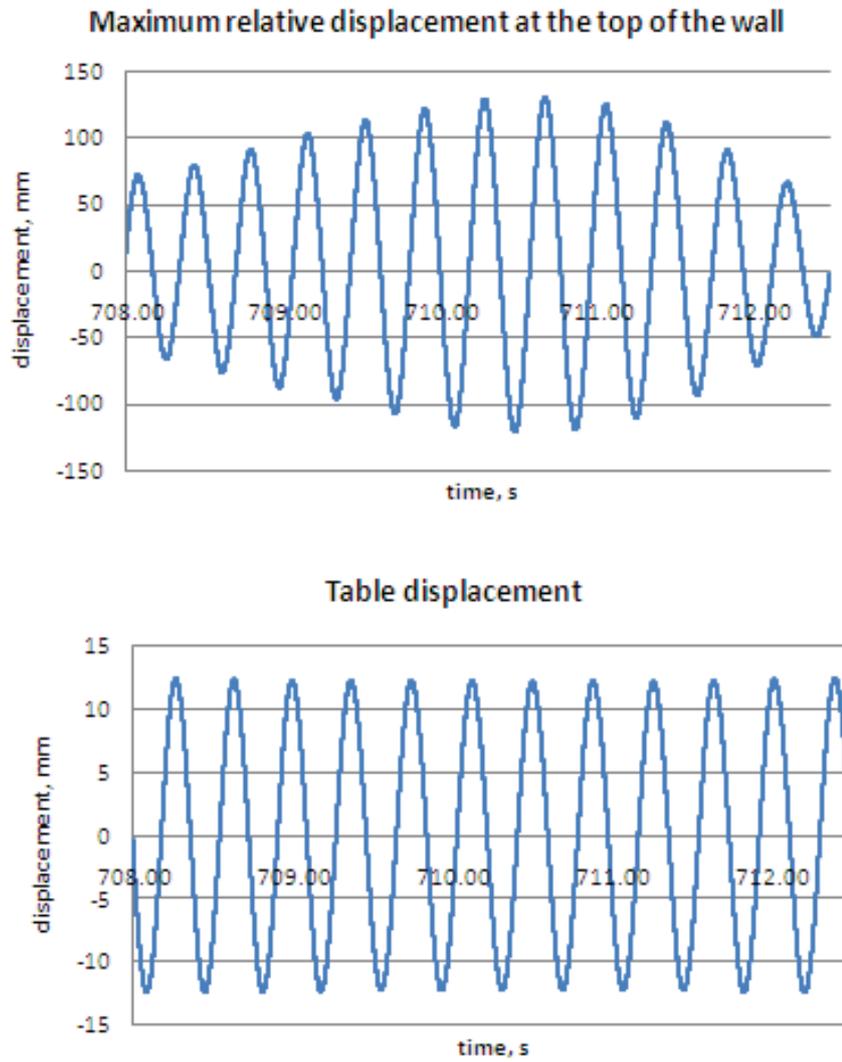
Fig 5.25 – Maximum relative displacement at the top of the wall and corresponding shake table displacement

Excitation 1. 8.65 Hz frequency.

Fig 5.26 – Displacement time histories at the top of the wall and shake table at excitation level 1

Excitation 2. 8.2 Hz frequency.
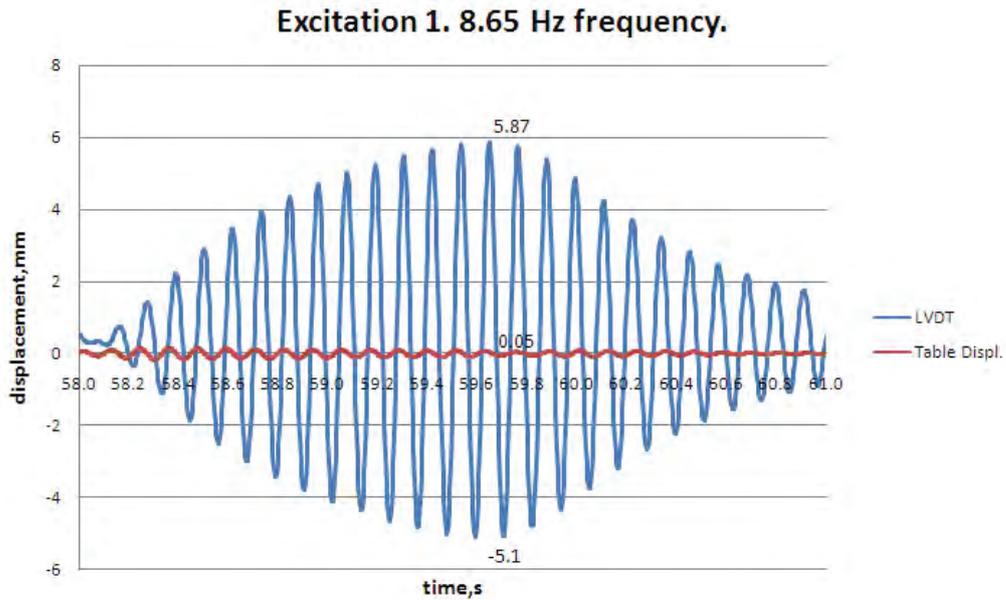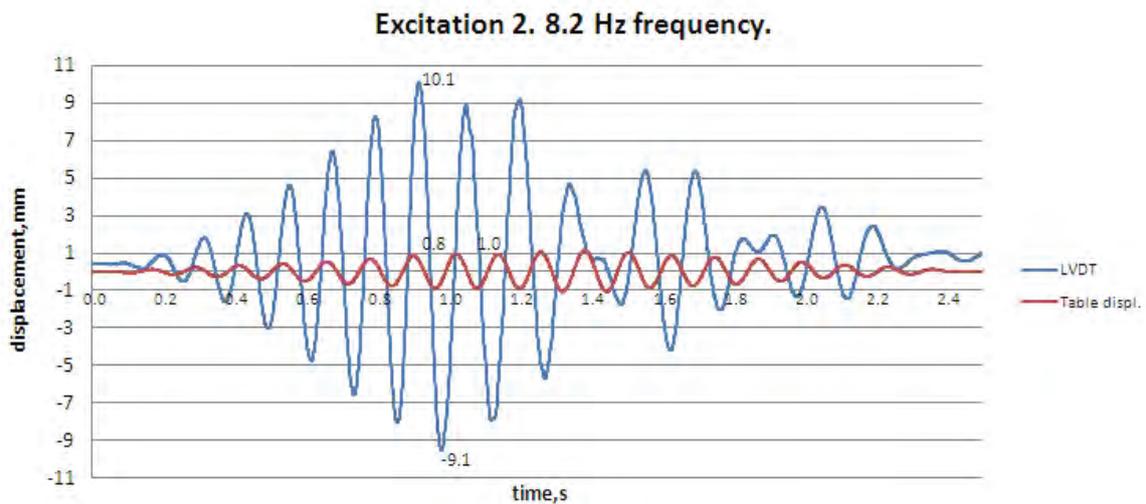
Fig 5.27 – Displacement time histories at the top of the wall and shake table at excitation level 2

Excitation 3. 7.2 Hz frequency.
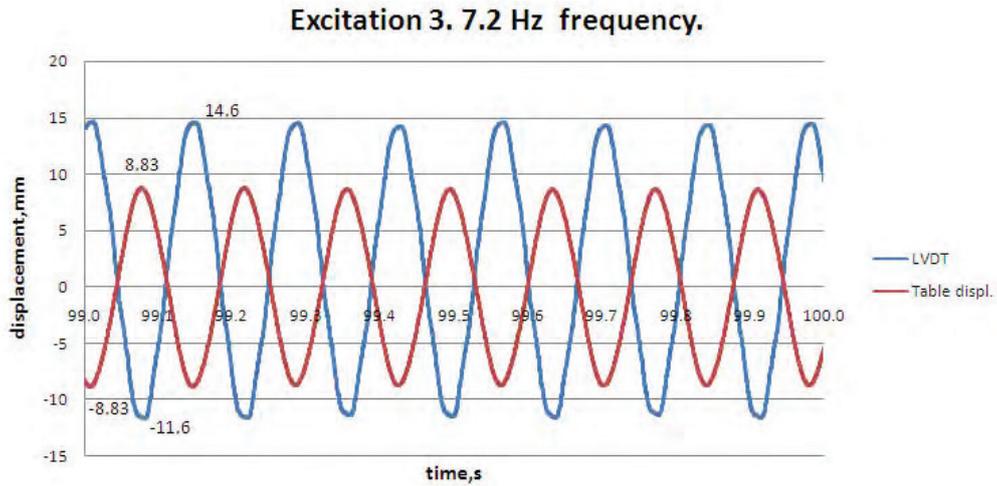
Fig 5.28 – Displacement time histories at the top of the wall and shake table at excitation level 3

Excitation 4. 5.7 Hz frequency.
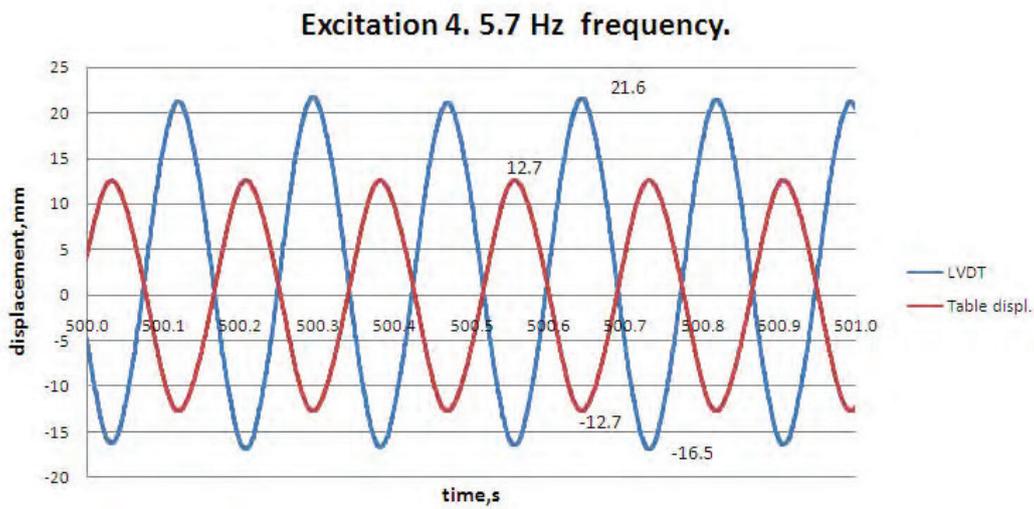
Fig 5.29 – Displacement time histories at the top of the wall and shake table at excitation level 4

Excitation 5. 3.6 Hz frequency.
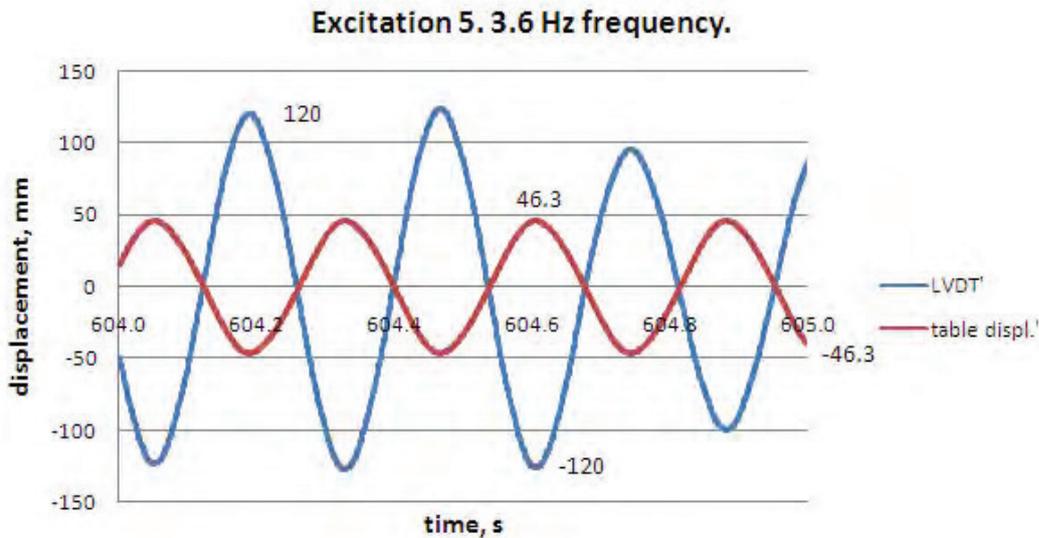
Fig 5.30 – Displacement time histories at the top of the wall and shake table at excitation level 5

The summary of results presented in Figures 5.24 to 5.30 are shown in Table 5.2 below, highlighting the ability of Dincel wall to undergo large deformations (up to 4.4% drift ratio). In this table "DMF" represents the corresponding value of Dynamic Magnification Factor.

No of experiment	Excitation 1	Excitation 2	Excitation 3	Excitation 4	Excitation 5	End of the test
DMF	15.9	6.7	1.3	1.14	3.85	-
Top rel. displ., mm	5.87	10.1	21.93	31.8	145	-
fn (at the beginning of the test), Hz	9.2 (h.t.)	8.04	7.44 (h.t.)	5.4	4.16	3.6 (h.t.)
ξ (at the beginning of the test), %	0.67 (h.t.)	0.94	1.21 (h.t.)	1.6	2.0	2.48 (h.t.)

(h.t.) - hammer test

Table 5.2 - Summary Table Dincel Wall

5.4.4 Response of the structure to dynamic excitation – Conventional wall

Frequency vs Maximum Displacement Graph combined for Excitations 1–4.

excitation 1, (fn=10.2Hz, ξ=1.18 % Uncracked State)

excitation 2, (fn=9.8 Hz, ξ=1.21 % Uncracked – Minor Cracked State)

excitation 3, (fn=4.43 Hz, ξ=1.4 % Major Cracked State)

excitation 4, (fn=2.84 Hz, ξ=1.6 % Major Cracked State)

after the test, (fn=2.37 Hz, ξ=1.7 % Major Cracked State)

Legend:

properties at the beginning of the excitation

excitation 1, (fn=10.2Hz, ξ=1.18 % Uncracked State)

- table displacement
- LVDT, top of the wall displacement
- relative displ. of the top of the wall to the table
- fn– instantaneous fundamental natural requency of the wall
- ξ– instantaneous damping ratio of the wall

Fig 5.31 – Frequency versus maximum displacement for four excitation states

Maximum relative displacement at the top of the wall

Table displacement
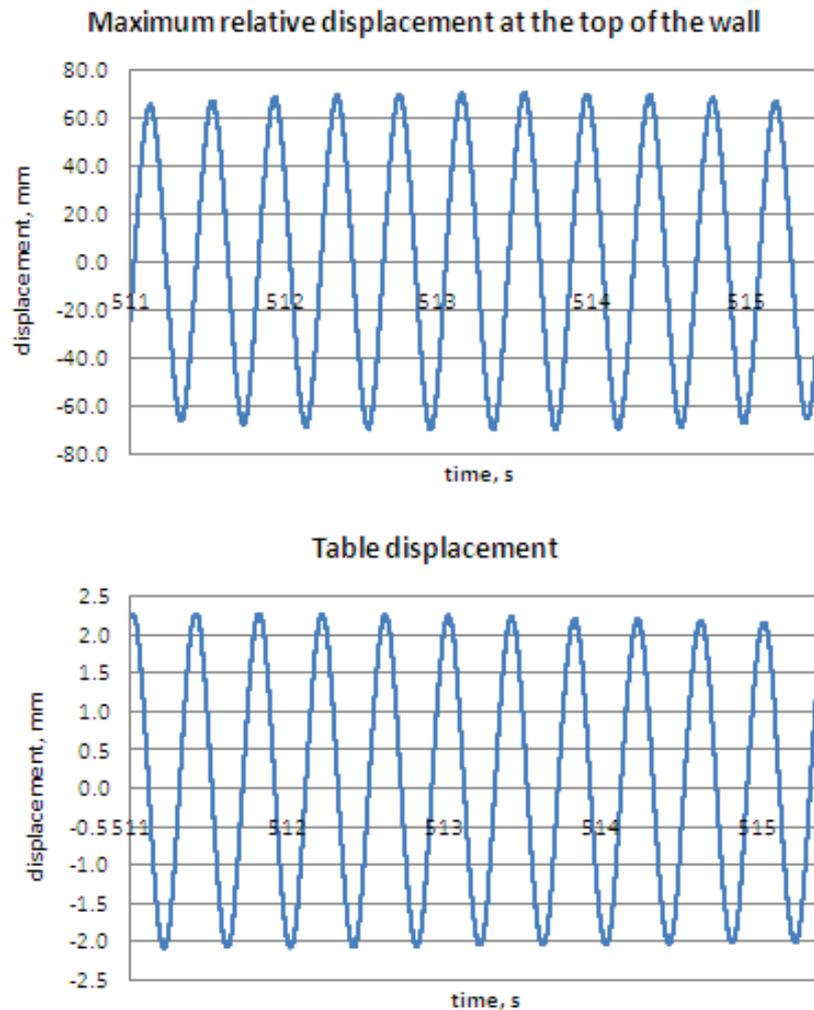
Fig 5.32 – Maximum relative displacement at the top of the wall and corresponding shake table displacement

Similar to Fig 5.25, Fig 5.31 conveys vital information in terms of maximum top displacement relative to shake table displacement for the conventional wall. We can see that as the first natural frequency drops due to increased severity of cracking, the relative displacement increases to a maximum value of 70 mm before the specimen was declared fully damaged and unsafe and the test stopped. This displacement value represented a storey drift of 2.1% (70/3,300) which is in the range of "near collapse" state based on Table 5.1 figures. This maximum displacement value is almost half of that displayed by Dincel wall, clearly

DINCEL
STRUCTURAL WALLING

demonstrating the superiority of Dincel wall to accommodate large displacement demands for a safe aseismic design.

In Fig 5.31, four stages of excitation and the corresponding responses are shown. For each stage, the corresponding frequency, damping ratio and maximum relative displacement are shown. Maximum relative displacement at the top of the wall is shown in fig. 5.32.

Displacement time histories at the top of the wall measured by a dynamic LVDT and those for the shake table are shown in Figures 5.33 to 5.36 for excitation levels 1 to 4, respectively.
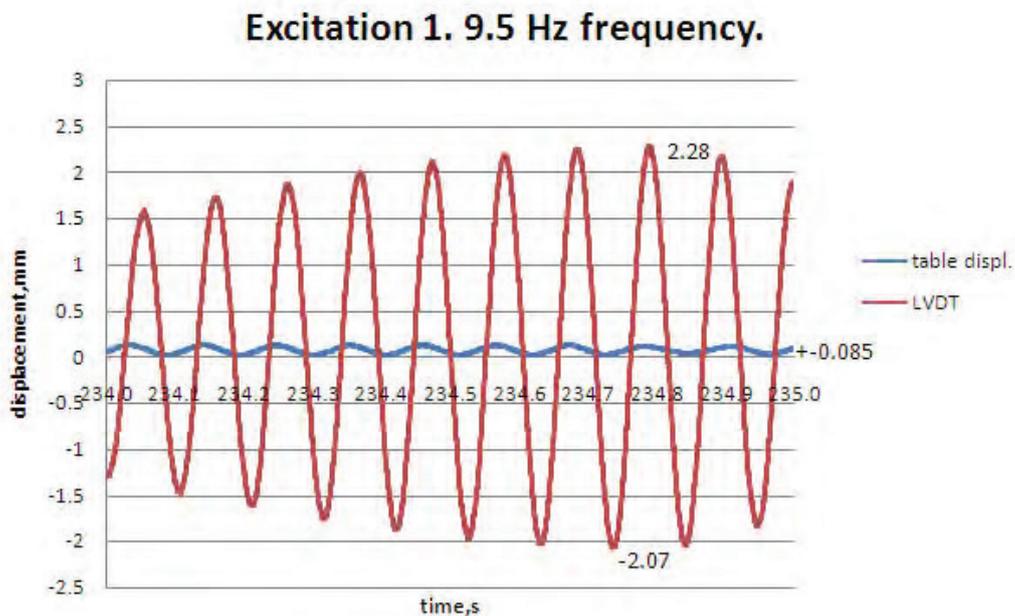
Fig 5.33 – Displacement time histories at the top of the wall and shake table at excitation level 1

Excitation 2. 6.85 Hz frequency.
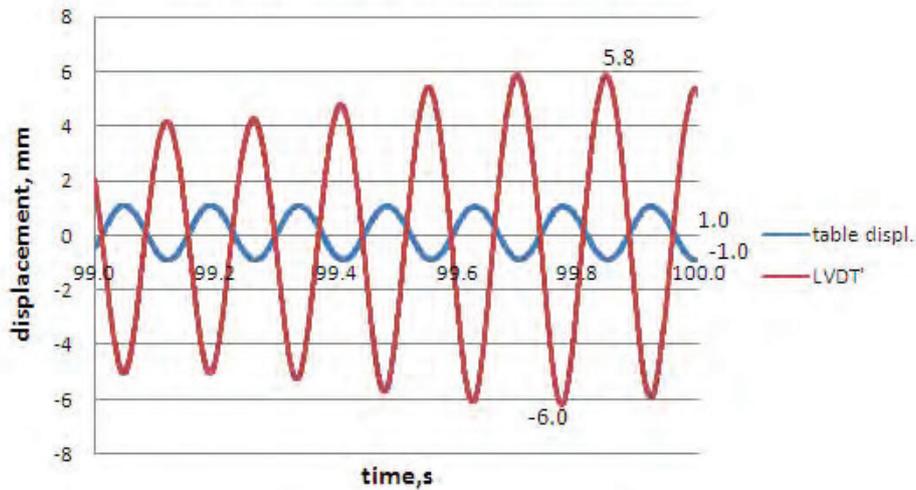
Fig 5.34 – Displacement time histories at the top of the wall and shake table at excitation level 2

Excitation 3. 3.5 Hz frequency.
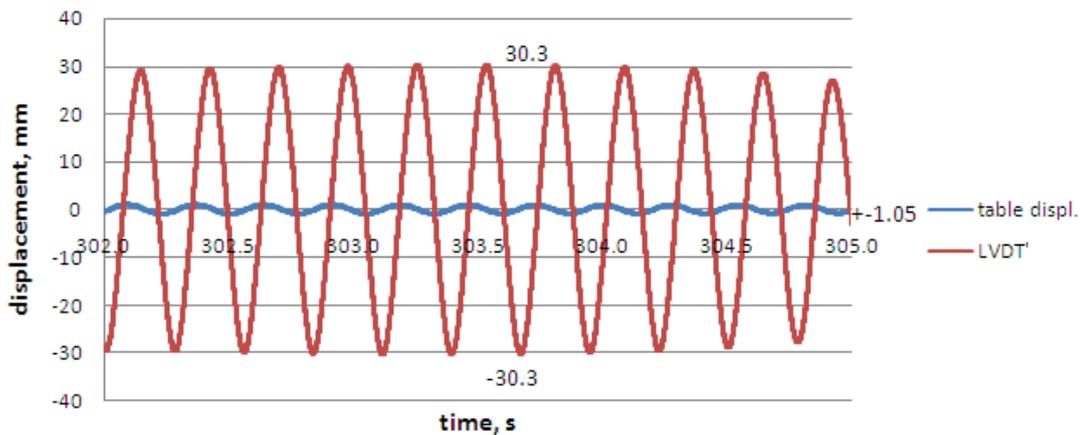
Fig 5.35 – Displacement time histories at the top of the wall and shake table at excitation level 3
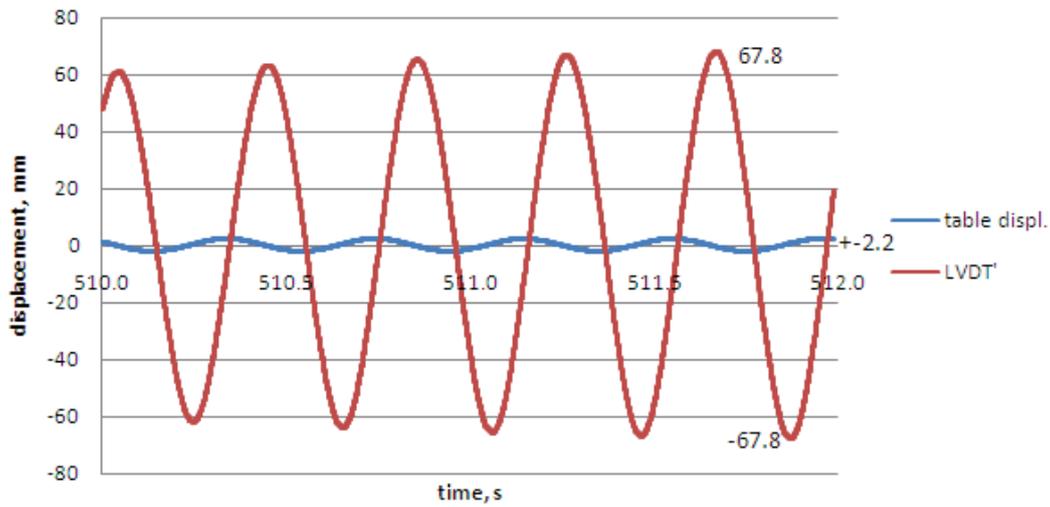
Fig 5.36 – Displacement time histories at the top of the wall and shake table at
excitation level 4

The summary of results presented in Figures 5.31 to 5.36 are shown in Table 5.3
below, highlighting the inability of the conventional wall to undergo deformations of
more than 2.1% drift ratio. In this table "DMF" represents the corresponding value
of Dynamic Magnification Factor.

*Comparison of the two specimens in terms of the top displacement is shown on fig.
5.37.*

Top Displacement of Dincel Wall (in blue) vs Conventional Wall (in red)
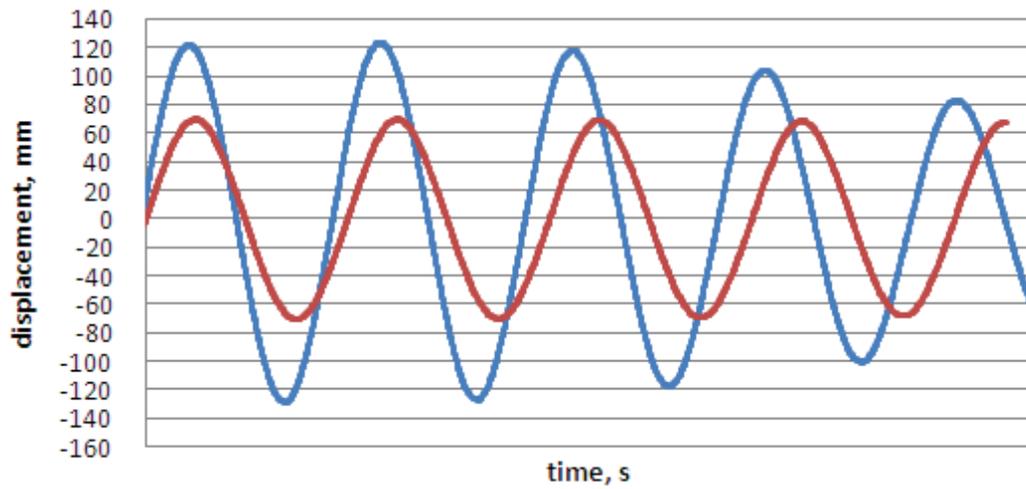
Fig 5.37 – Comparison of the top displacement of both walls

No of experiment	Excitation 1	Excitation 2	Excitation 3	Excitation 4	End of the test
DMF	15.5	7.1	24.02	22.3	-
Top rel. displ., mm	2.28	6.9	31.35	70.0	-
fn (at the beginning of the test), Hz	10.2(h.t.)	9.8(h.t.)	4.43	2.84	2.37(h.t.)
ξ (at the beginning of the test), %	1.18(h.t.)	1.21(h.t.)	1.47	1.5	1.7(h.t.)

(h.t.) – hammer test

Table -5.3 Summary Table Conventional Wall

Finally Table 5.4 compares the results of Table 5.2 and Table 5.3.

Type of wall	Dincel	Conventional	Design calculation
Initial first natural frequency fn, Hz	9.2	10.2	10.88
Initial damping ratio ξ, %	0.67	1.18	0.5
Initial stiffness k, kN/m	3,941	4,844	5,504
Top wall displ. Relative to the table before first crack occurred: test value/theoretical value	9.6/6.6	5.8/5.37	4.73
Max. top wall displ. relative to the table, mm/table displ., mm /magnification factor DMF	145/25/3.85	70/2.2/22.3	n/a
Drift %	4.4	2.1	n/a
First natural frequency after the test fn, Hz	3.6	2.37	n/a
Damping ratio after the test ξ, %	2.48	1.7	n/a
Stiffness after the test k, kN/m	604	262	n/a

Table 5.4 - Comparison of results between Dincel wall and the conventional wall

6   Strength of Flexural Members

Although the main objective of this document is to report on analysis and testing of shear wall systems in resisting large scale earthquake forces, the strength of flexural Dincel members (ie beams) is also of interest as flexural members, to some extent, also participate in resisting portion of seismic forces.

In this section the results of a comprehensive set of flexural tests on Dincel beams and ordinary reinforced concrete beams is reported and compared. The information presented in this section is only a small part of the original study. The full report can be obtained from Dincel Construction System Pty Ltd.

6.1   Objectives and Scope

3400 mm lengths of Reinforced and Unreinforced Dincel and Conventional Reinforced Concrete samples would be tested using a standard four point loading test. The tests were performed at the UTS Concrete Laboratory.

In order to demonstrate the additional strength and ductility of Dincel beams in comparison to conventional concrete, 9 different samples were tested as shown in Table 6.1.

Testing Sample	Number of samples tested
Conventional Reinforced Concrete	3
Reinforced Dincel	3
Unreinforced Dincel	3

Table 6.1 – Samples tested

The Conventional Reinforced Concrete and Dincel samples had identical reinforcement.

6.2 Definition of the Testing Samples

Conventional Reinforced Concrete: A reinforced concrete sample consisting of 1N12 bar. The reinforcing bar was placed with 35 mm clear cover from the bottom tension face, each sample having a depth of 200 mm and a width of 364 mm.

Reinforced Dincel: A reinforced concrete sample formed and tested inside a Dincel P-1 polymer profile. The sample having 1N12 bar placed with 35mm clear cover from the bottom tension face, each sample having a depth of 200 mm and a width of 364 mm.

Unreinforced Dincel: An unreinforced concrete sample formed and tested inside a Dincel P-1 polymer profile, each sample having a depth of 200 mm and a width of 364 mm.

6.3 Construction of Testing Samples

There were a total of 6 reinforced test samples including:

- 3 Conventional Reinforced Concrete samples
- 3 Reinforced Dincel samples

Each of these samples had one steel reinforcement bar placed at mid section. The reinforcement bar was an N grade reinforcement bar of 12mm in diameter (1N12). For strain readings of the steel reinforcement during testing, electrical strain gauges were used.

For the three Conventional Reinforced Concrete samples, it was decided to provide the same external profile as the reinforced Dincel walls in order to achieve similarity of samples. Constructing the samples in this way would allow for a more direct comparison between the Dincel and Conventional Reinforced Concrete samples.

DINCEL
STRUCTURAL WALLING

6.4 Four Point Loading Tests

All 9 samples were subjected to four point loading tests subjecting the specimens to two equal vertical loads at 1/3 span lengths resisted by two equal reactions at the beam ends. The load-displacement of all beams were measured by load cells and a linear variable displacement transducer (LVDT) as shown in Fig 6.1 and 6.2.

Fig 6.1 – Linear variable displacement transducer (LVDT) measuring displacement at mid span of the beam

Figure 6.2 – Front of testing platform

6.5   Test Procedure

For each set of tests the following loading regimes were adopted.

Loading regime for Conventional Reinforced Concrete Samples and Reinforced Dincel Samples

1. Load up to 50% of theoretical maximum external load = 6.30 KN
2. Unload
3. Load up to 75% of theoretical maximum external load = 9.45 KN
4. Unload
5. Load up to the maximum load the sample can withstand.
6. Unload
7. Load until maximum load again.

Loading Regime for Unreinforced Dincel Samples

1. Load up to 50% of assumed maximum load = 12 KN
2. Unload
3. Load up to 75% of assumed maximum load = 18 KN
4. Unload
5. Load up to the maximum load the sample can withstand.
6. Unload
7. Load until maximum load again.

Upon applying the load, the beams start to deform and cracks start to also appear as seen in Fig 6.3 and 6.4, until complete failure as seen in Fig 6.5. Figure 6.6 shows the load – deformation curve for sample 1 of Reinforced Dincel beam. Figure 6.7 shows the load – deformation comparison between the 3 Conventional Reinforced Concrete samples and the 3 Reinforced Dincel samples. As can be seen from the figure the Dincel beam displays large ductility and capacity for large deformations which is vital for seismic applications.

Fig 6.3 – Flexural cracks in Conventional Reinforced Concrete Beam Specimen

Fig 6.4 – Large flexural cracks developing in Conventional Reinforced Concrete Beam Specimen

Fig 6.5 - Conventional Reinforced Concrete Beam Specimen after failure
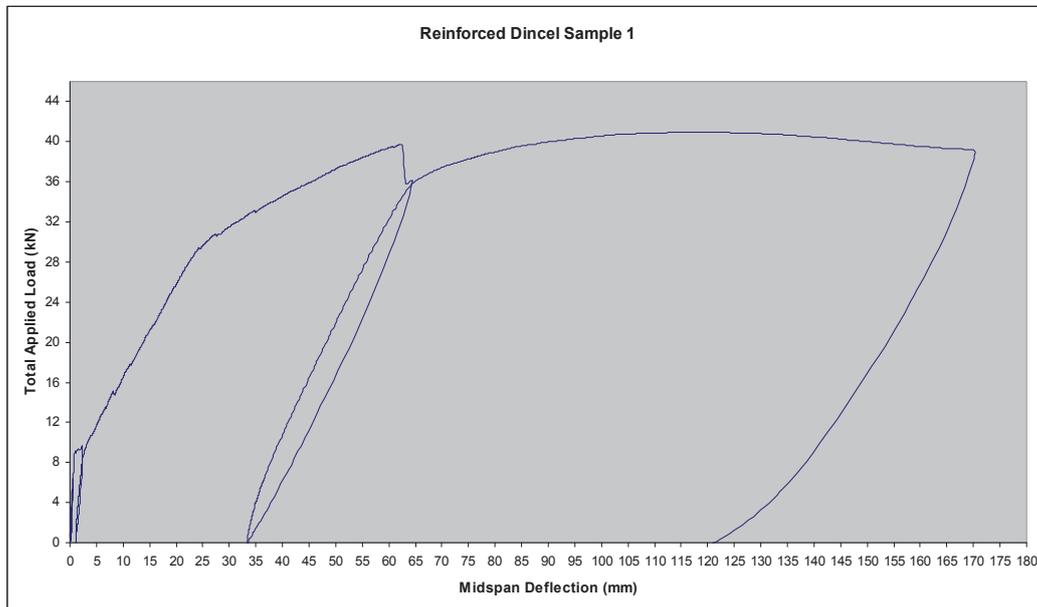
Figure 6.6 - Total applied load vs midspan deflection for Reinforced Dincel sample 1
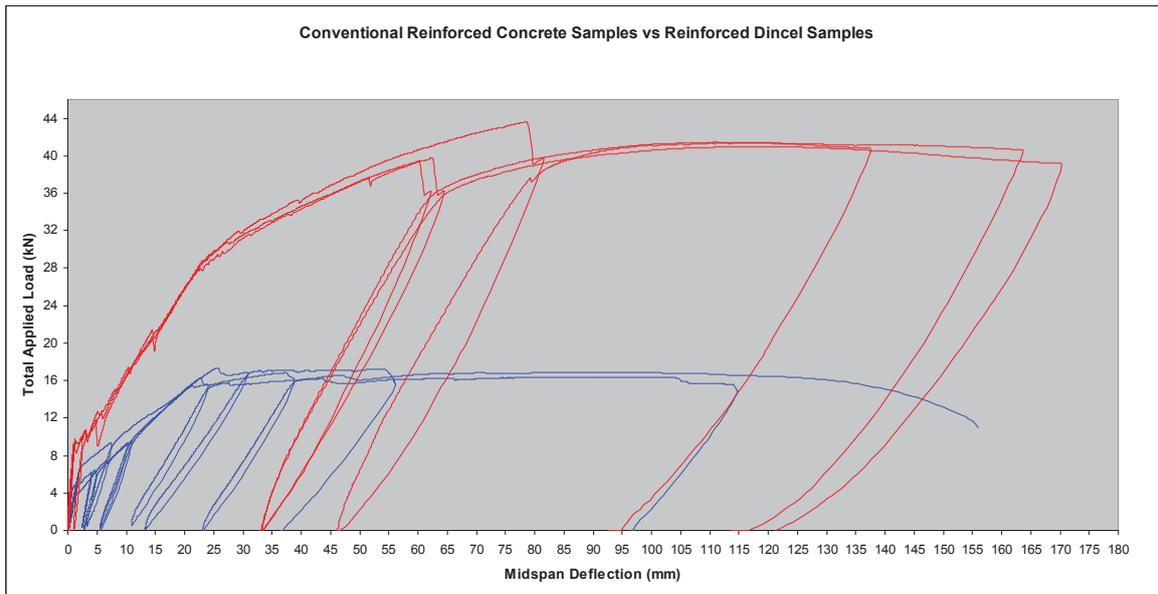
Figure 6.7 – Total applied load vs midspan deflection comparison between

Conventional Reinforced Concrete samples (IN BLUE) and Reinforced Dincel samples

6.6   Test Results

Table 6.2 summarises the total maximum load carried by each sample. As can be seen from Table 6.2, the Reinforced Dincel samples carried **2.5** times the load the Conventional Reinforced Concrete samples carried. The Unreinforced Dincel samples carried **1.4** times the load the Conventional Reinforced Concrete samples carried. These results clearly demonstrate the load carrying superiority of Dincel over conventional Reinforced Concrete beams.

Sample	Maximum Load (kN)
Conventional Reinforced Concrete Samples	
1	17.35
2	16.33
3	16.86
AVERAGE	**16.85**
Reinforced Dincel Samples	
1	40.95
2	41.45
3	43.60
AVERAGE	**42.00**
Unreinforced Dincel Samples	
1	22.34
2	24.48
3	23.31
AVERAGE	**23.38**

Table 6.2 – Summary of total maximum load withstood by each sample

7   Conclusions

The series of tests and accompanying analysis, either simple analysis or more sophisticated Finite element analyses, have confirmed the suitability of Dincel system to resist large lateral forces and resulting displacement caused by major ground motions measuring 8.5 and over on the Richter scale. Hence Dincel system offers a safe and practical system and a reliable seismic resistant solution.

The tests conducted at the Structures Laboratory at the University of Technology Sydney included testing two large scale u-shaped panels in "in-plane" loading and confirming the ability of the Dincel wall system to act as effective shear wall system by accommodating the required inter-storey drifts caused by large past earthquakes (eg the 1995 Kobe Earthquake in Japan). These tests were then complemented by a series of dynamic tests conducted on UTS shake table subjecting two separate specimens to large displacements by creating near resonance conditions under sinusoidal motions. The cantilever specimens, 4.0 m in length and 640 mm in width and 195 mm in depth were subjected to varying motion amplitude and frequency to ensure near resonance conditions at all times.

The specimen sample "D" made up of conventional concrete displayed a maximum top displacement of 70 mm (deformation level of 2.1%) before being declared as unsafe while a similar specimen made up of Dincel system was able to demonstrate a maximum top displacement of 145 mm (deformation level of 4.4%) before being declared as unsafe.

A ratio of more than 2 to 1 in accommodating large displacement is a testimony to Dincel Walls' superiority as an effective aseismic system. The lateral stiffness of Dincel Wall system is the equivalent of a comparable conventional plain concrete wall. Furthermore, the confinement offered by the polymer encapsulation is vital in maintaining stiffness and delaying its deterioration, hence resulting in much safer structures in terms of preservation of life and preventing collapse.

The author has no reservation in recommending the system to the global community on the basis of its proven performance under most hostile loading environments.

DINCEL
STRUCTURAL WALLING

8   References

Ansys Inc. SAS IP (2005), *11.0 Documentation for ANSYS*

Australian Standards, Structural Design Actions (2007) AS/NZS 1170.4 *Part 4 - Earthquake Actions in Australia*

Australian Standard (2009), AS 3600

Bolton, A.– *Natural frequencies of structures for designers -The Structural Engineer/September 1978/No.9/Volume 56A* – Heriot Watt University, Edinburgh

Cook, R. D. (1995) *Finite Element Modelling for Stress Analysis,* John Wiley & Sons Inc, New York.

Dincel Construction System Pty Ltd, *Dincel Construction Manual, January 2010 – Revision 10,* Parramatta NSW.

MacLeod, I.A. (2005) *Modern Structural Analysis – Modelling Process & Guidance,* Thomas Telford Books, London.

Rombach, G.A. (2004) *Finite Element Design of Concrete Structures,* Thomas Telford Books, London.

Appendix A – Reinforcement Details of Earthquake Wall Samples

- **Drawing for unreinforced, i.e. non-shear Dincel Wall connection to floor slabs**

- **Drawings for U-shaped panel samples A and B**
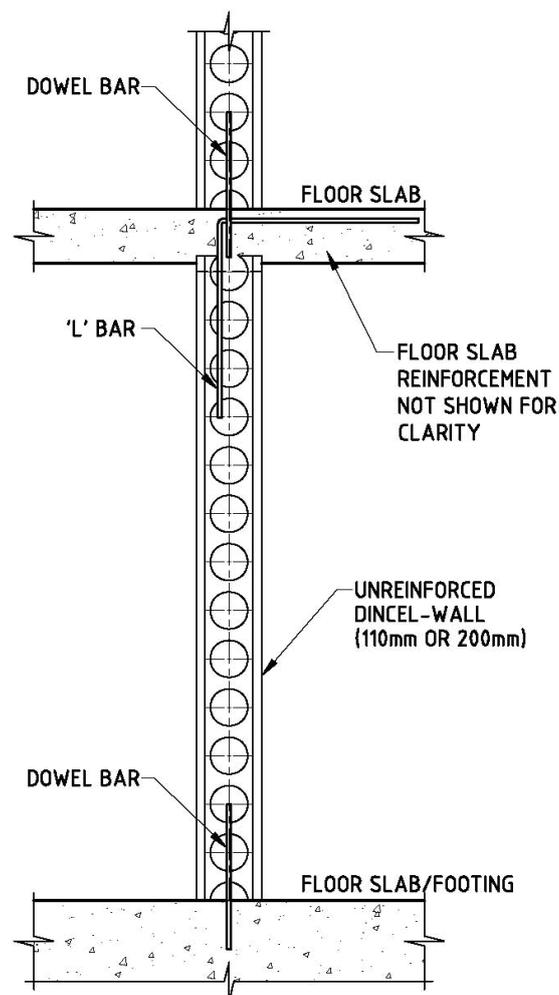
Figure A.1 Unreinforced Dincel Wall Floor Slab Connection to Prevent Walls From Falling During an Earthquake Event

SECTION 2
SCALE 1:20

N12-666 STARTER BAR (J)

200
2800

SAMPLE B
UN-REINFORCED SPECIMEN

PLYWOOD SHUTTER
1N20 BAR (F) IN CORNER
N12-600 BAR (E)
P-1
P-J
P-CF
P-EC
P-3
333
333
55
25
200
N12-600 BAR (E)
1N20 BAR (F) IN CORNER
PLYWOOD SHUTTER
P-J
P-CF
P-EC
25
55
333
333
200

SECTION 1
SCALE 1:20

N16-300 HORIZ. BAR (C)
N16-VERT BAR (D)
N16-333 STARTER BAR (G)
200
2800

SAMPLE A
REINFORCED SPECIMEN

N16-300 BAR (A)
PLYWOOD SHUTTER
ALL VERTICAL REINFORCEMENT TO BE N16 BARS
N16-300 BAR (B)
N16-VERT. BAR (D)
N16-300 BAR (C)
P-1
P-J
P-CF
P-EC
P-3
LAP 800
333
333
55
25
200
2977
N16-300 BAR (A)
PLYWOOD SHUTTER
P-1
P-J
P-CF
P-EC
25
55
333
333
200

• F'c 28 DAYS = 32MPa
• 10mm AGGREGATE
• 100mm SLUMP AT THE POINT OF DISCHARGE

STARTER BAR PLACEMENT SAMPLE B

STARTER BAR PLACEMENT SAMPLE A

STARTER BAR PLACEMENT SAMPLE A

STARTER BAR SCHEDULE

REINF. BAR	QUANTITY	BAR SIZE
G	17	N16-333
H	2	N20
J	6	N12-666

REINFORCEMENT SCHEDULE

REINF. BAR	QUANTITY	BAR SIZE
A	18	N16-300
B	9	N16-300
C	9	N16-300
D	19	N16 VERT.
E	20	N12-600
F	2	N20 VERT.

N20 STARTER BAR (H) IN CORNER

N12-666 STARTER BAR (J) TYP.

N20 STARTER BAR (H) IN CORNER

N16-333 STARTER BAR (G)

REINF. BAR – A
REINF. BAR – B
REINF. BAR – C
REINF. BAR – D
REINF. BAR – E
REINF. BAR – F
REINF. BAR – G
REINF. BAR – H
REINF. BAR – J

TOP OF TEST BASE

Title Block

DRAWING TITLE: REINFORCEMENT BAR DETAILS AND SCHEDULE

DRAWING No. 01061-LST2

SCALE 1:20 DATE APR '09 DRAWN MH

dincel & associates
consulting structural & civil engineers
7K Parkes Street, Parramatta, NSW 2150,
Phone: (02) 9689 1877 Fax: (02) 9689 2026
Email: dincel@dincel.com.au

SUB-CONSULTANT

PROJECT: EARTHQUAKE TESTING PROGRAM WALL SAMPLES

CLIENT: DINCEL CONSTRUCTION SYSTEM

DESIGNED: BURAK DINCEL B.E.M. ENG. Sc. M.I.E.AUST. C.P.ENG.

CHECKED: ALAN HAMILTON B.E.(HONS) M.I.E.AUST. C.P.ENG. NPER

APPROVED BY, FOR AND ON BEHALF OF DINCEL & ASSOCIATES

CHARTERED MEMBER

THIS DRAWING IS NOT FOR CONSTRUCTION, UNLESS SIGNED BY THE DESIGN ENGINEER

USE OF THESE DRAWINGS
THESE DESIGN AND DETAILS SHOWN ON THESE DRAWINGS ARE APPLICABLE TO THIS PROJECT ONLY AND MAY NOT BE REPRODUCED IN WHOLE OR IN PART OR BE USED FOR ANY OTHER PROJECT OR PURPOSE WITHOUT THE WRITTEN PERMISSION OF DINCEL & ASSOCIATES WITH WHOM COPYRIGHT RESIDES.

SPECIMEN SAMPLE – 'C'

SECTION 2
SCALE 1:10

666
640mm CONCRETE
200
195mm CONCRETE
19 mm PLYWOOD EACH END

2N16 BARS CENTRE FOR LIFTING AND SAFETY PURPOSES DURING TESTS

CONCRETE SPECIFICATION:
F'c = 32 Mpa
SLUMP : 120 mm
MAX. AGGREGATE SIZE : 10mm

SECTION 1
SCALE 1:20

4000
200
TESTING SUPPORT FRAME

DINCEL WALL ELEVATION
SCALE 1:20

2 OFF φ13 mm CONDUITS (FOR LIFTING PERPOSES)

2 OFF φ13 mm CONDUITS (FOR TEST SUPPORT FRAME)
TESTING SUPPORT FRAME

2 OFF φ13 mm CONDUITS (FOR TEST SUPPORT FRAME)
TESTING SUPPORT FRAME

666
150
700
2500
4000

DESIGNED BURAK DINCEL
B.E. M.EngSc M.I.E. AUST. C.P.Eng. RPEQ NPER
CHECKED ALAN HAMILTON
B.E.(HONS) M.I.E. AUST. C.P.ENG. NPER
APPROVED BY, FOR AND ON BEHALF OF DINCEL & ASSOCIATES
MEMBER

PROJECT
DINCEL CONSTRUCTION SYSTEM
EARTHQUAKE TESTING STAGE 2

CLIENT
DINCEL CONSTRUCTION SYSTEM

dincel & associates
consulting structural & civil engineers

7K Parkes Street
Parramatta, NSW 2150.
Phone: (02) 9689 1877
Fax: (02) 9689 2028
Email: dincel@dincel.com.au

SUB-CONSULTANT

DRAWING TITLE
EARTHQUAKE WALL SAMPLES
REINFORCEMENT DETAILS SAMPLE 'C'

DRAWING No.
01061-LST3

SCALE 1:20, 1:10
DATE JUNE '10
DRAWN MH

access:UTS

SECTION 2
SCALE 1:10

SPECIMEN SAMPLE - 'D'

196
642

2N16 BARS CENTRE
FOR LIFTING AND
SAFETY PURPOSES
DURING TESTS

CONCRETE SPECIFICATION:
F'c = 32 Mpa
SLUMP : 120 mm
MAX. AGGREGATE SIZE : 10mm

TESTING SUPPORT FRAME

4000
195

SECTION 1
SCALE 1:20

DINCEL WALL ELEVATION
SCALE 1:20

2 OFF Ø13 mm CONDUITS
(FOR LIFTING PERPOSES)

2 OFF Ø13 mm CONDUITS
(FOR TEST SUPPORT FRAME)

TESTING SUPPORT FRAME

2 OFF Ø13 mm CONDUITS
(FOR TEST SUPPORT FRAME)

TESTING SUPPORT FRAME

640
150
700
2500
4000

DESIGNED BURAK DINCEL
B.E. M.Eng.Sc.M.IE.Aust. C.P.Eng. RPEQ.NPER

CHECKED ALAN HAMILTON
B.E. (HONS) M.I.E.AUST. C.P.ENG. NPER

APPROVED BY, FOR AND ON BEHALF OF
DINCEL & ASSOCIATES
CHARTERED
MEMBER

PROJECT
DINCEL CONSTRUCTION SYSTEM
EARTHQUAKE TESTING STAGE 2

CLIENT
DINCEL CONSTRUCTION SYSTEM

dincel & associates
consulting structural & civil engineers

7K Parkes Street
Parramatta, NSW 2150.
Phone: (02) 9689 1877
Fax: (02) 9689 2028
Email:dincel@dincel.com.au

SUB-CONSULTANT

DRAWING TITLE
EARTHQUAKE WALL SAMPLES
REINFORCEMENT DETAILS SAMPL 'D'

DRAWING No.
01061-LST4

SCALE 1:20, 10
DATE JUNE '10
DRAWN MM

DINCEL
STRUCTURAL WALLING

Appendix B – Calculation of Wall Properties and Characteristics

In order to obtain real values for dynamic properties of the wall, calculation is done with a safety factor = 1
Safety factor γ= 1.5 is taken for the calculation of maximum force acting from the wall to the supporting structure.
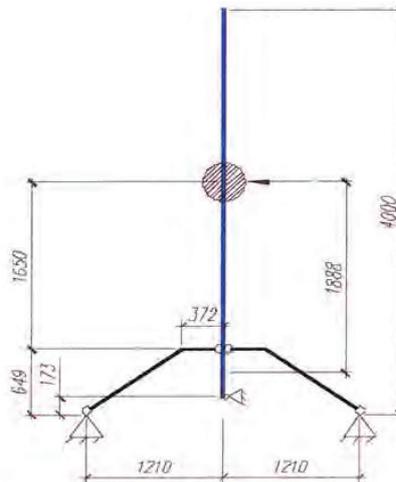
Design model of the testing setup

Properties of the wall are the following:

Concrete:

$f'c=$	32	(Mpa; characteristic compressive strength, design)
$f'cfact=$	65	(Mpa; factual characteristic compressive strength at the test day)
$f'ct.f=$	3.39	(Mpa; tensile strength, design)
$f'ct.ffact=$	4.84	(Mpa; factual tensile strength at the test day)

Section properties:

$h=$	0.666	(m; section height)
$w=$	0.20	(m; section width)
$W=$	0.00444	(m^3; section moment of area)

Maximum moment at the base of the wall for uncracked condition of the wall (f'ct.f value used):

$$M_{max} = Wf'_{ct.f} = \quad 15.1 \quad (kNm)$$

Maximum moment at the base of the wall for uncracked condition of the wall (f'ct.f.fact. value used):

$$M_{max}^{fact} = Wf'_{ct.f.fact} = \quad 21.5 \quad (kNm)$$

Maximum moment which may act at the base of the wall (for the calculation of the force acting on supports):

$$\max M = Wf'_{ct.f.fact} \cdot \gamma = \quad 32.2 \quad (kNm)$$

Dynamic mass of a single degree of freedom system representing the wall (*see picture above*):

$$m = (L + 1.65) \cdot bw \cdot \gamma = 1179 \quad (kg) = \quad 11.55 \quad (kN)$$

Distance from the center of the base to the center of the mass (*see picture above*):

$$L= 1.89 \quad (m)$$

Max shear allowed on the wall section for uncracked condition (design value):

$$V=Mmax/L= 8.0 \quad (kN)$$

Stiffness of conventional wall:

$E(32Mpa)$= 30100   _(Mpa; modulus of elasticity) - AS3600_

I= 0.00041153   _(m^4 ; second moment of area)_

A= 0.1332   _(m^2 ; cross-sectional area)_

EI= 12387   _(kNm^2)_

EA= 4009320   _(kN)_

$k=3EI/L^3$= 5504   _(kN/m; stiffness of 1 DOF cantilever structure)_

Dynamic properties of 1 DOF system (cantilever wall):

ξ= 0.5   _(%; assumed damping ratio for the wall)_

$T_d = 2\pi\sqrt{\dfrac{m}{k}} / \sqrt{(1-\xi^2)} =$ 0.092   _(s; damped period of vibration)_

$f_d = 1/T_d =$ 10.88   _(Hz; damped natural frequency)_

$w_d = 2\pi f_d =$ 68.3   _(rad/s; damped cyclic frequency)_

Parameters of excitation A:

$\bar{f} = 10.10$ _(Hz)_   =   <u>0.93</u> _fn_   _(frequency of excitation)_

a= 0.09   _(g)=_   0.89 _m/s2_   _(acceleration of excitation)_

u_{max} = <u>0.22</u>   _(mm; amplitude of excitation)_

$\beta \equiv \dfrac{\bar{\omega}}{\omega} = 0.93$ _(ratio of the applied frequency of excitation to the natural frequency of the wall)_

D= 7.25   _(dynamic magnification factor)_

ma= 1.04   _(kN; mass x acceleration)_

$V=maD$= 7.58   _(kN)_   <   _Vmax=_   8.0   kN   _(dynamic response)_

                       OK   <u>section remains uncracked</u>

Parameters of excitation B:

$\bar{f} = 7.60$ _(Hz)_   =   <u>0.70</u> _f_   _(frequency of excitation)_

a= 0.23   _(g)=_   2.28 _m/s2_   _(acceleration of excitation)_

u_{max} = <u>1.00</u>   _(mm; amplitude of excitation)_

$\beta \equiv \dfrac{\bar{\omega}}{\omega} = 0.70$ _(ratio of the applied frequency of excitation to the natural frequency of the wall)_

D= 1.95   _(dynamic magnification factor)_

ma= 2.69   _(kN; mass x acceleration)_

maD= 5.25   _(kN)_   <   _Vmax=_   8.0   kN   _(dynamic response)_

                       OK   <u>section remains uncracked</u>

Appendix C - Forces Acting on each Element, Calculated using Finite Element Analysis

Base shear maxV=   17.0
Base moment maxM=   32.2
Results obtained:

1. Design diagram

Loading 1
Diagram N
Units of measurement - T

Minimum force -2.49626
Maximum force 2.49626

2. Axial Forces N, kN

2.23   2.23   2.496
-2.23 -2.496   -2.23
-2.496
2.496
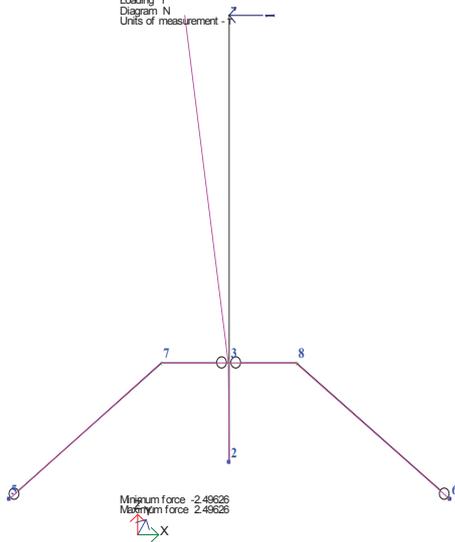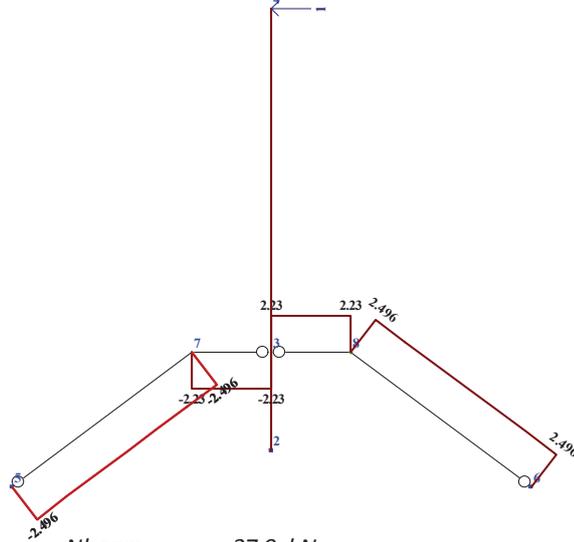
Nbeam=   37.9 kN
Nsupport=   42.4 kN

3. Shear Forces, kN

Loading 1
Diagram My
Units of measurement - T*M

1.198   1.198   0.417
-0.417
-1.198   -1.198
-3.459
-3.459
0.417
-0.417

Minimum force -0.443148
Maximum force 1.65
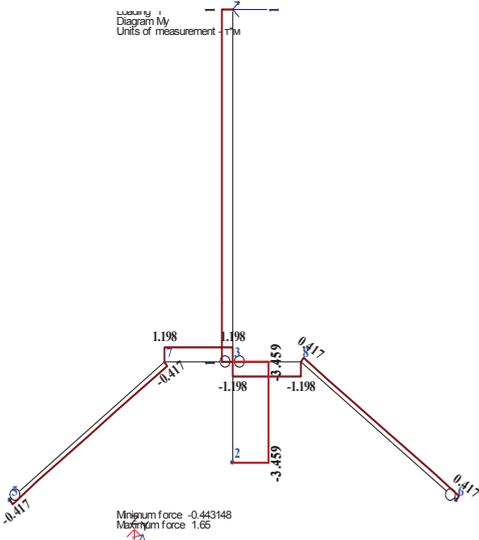
Qbeam=   20.4 kN
Qsupport=   7.1 kN

4. Bending Moments, kNm

-0.443 -0.443
1.65
0.443
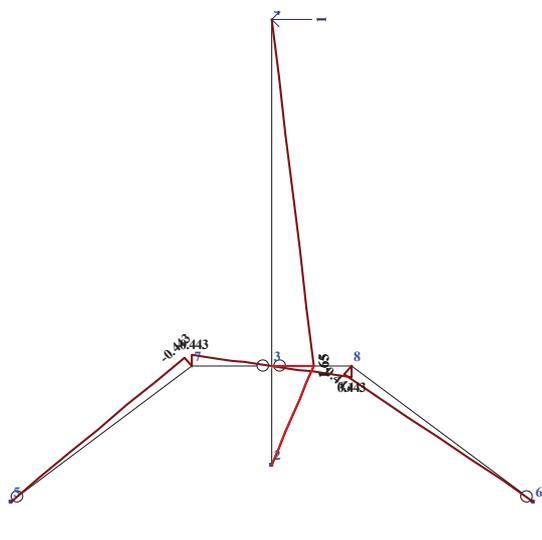
Mbeam=   7.5 kNm
Msupport   7.5 kNm